

Optimistic limits of colored Jones polynomials and complex volumes of hyperbolic links

JINSEOK CHO

March 18, 2013

Abstract

A combinatorial definition of the optimistic limit of Kashaev invariant was suggested by the author and others. This new definition was easy to handle and had natural geometric meaning for any hyperbolic link diagrams. On the other hand, it was known that the Kashaev invariant coincides with the colored Jones polynomial evaluated at a certain root of unity. Therefore, it is very natural to apply the defining method to the colored Jones polynomials.

In this article, we suggest a combinatorial definition of the optimistic limit of the colored Jones polynomial and show that it determines the complex volume of a hyperbolic link. Furthermore, we show that this optimistic limit coincides with the optimistic limit of the Kashaev invariant modulo $4\pi^2$.

1 Introduction

The optimistic limit of Kashaev invariant was first appeared in [5] when Kashaev suggested the volume conjecture, and it was formulated and developed by several others in [7], [4] and [11]. Recently, the author with H. Kim and S. Kim suggested a modified definition of the optimistic limits for any hyperbolic link diagrams in [1] and showed they determine the complex volumes of the links. Comparing to previous definition, this new definition in [1] was easy to handle and had natural geometric meaning. (We will summarize the results of [1] in Section 5.)

On the other hand, it was proved in [8] that

$$J_L(N; \exp \frac{2\pi i}{N}) = \langle L \rangle_N,$$

where $\langle L \rangle_N$ is the N -th Kashaev invariant of a link L and $J_L(N; x)$ is the N -th colored Jones polynomial of L with a complex variable x . Therefore, it is natural to define the optimistic limit of the colored Jones polynomial so that it determines the complex volume. Although it looks trivial, there are several issues related to the ambiguity of the optimistic limit. See Section 1.1. of [2] for details of the meaning of the optimistic limit and the related issues.

The optimistic limit of the colored Jones polynomial was formulated and developed in [9], [3] and [2]. Especially, the author and J. Murakami suggested a method to define the optimistic limits of the colored Jones polynomials of general hyperbolic knots in [2] and showed they determine the complex volumes. However, this method was very delicate and complicated. Hence we suggest a new definition in this article using the idea of [1]. This new definition shares the same advantages of the definition in [1], namely it works for any hyperbolic links, it is more intuitive, easy to handle and has natural geometric meaning.

The optimistic limit of the colored Jones polynomial is defined using the potential function $W(w_1, \dots, w_n)$, which is defined combinatorially from an oriented diagram D of a hyperbolic link L . This function will be defined in Section 2. Then we consider the following set of equations

$$\mathcal{I} := \left\{ \exp \left(w_k \frac{\partial W}{\partial w_k} \right) = 1 \mid k = 1, \dots, n \right\}. \quad (1)$$

In Section 3, we introduce an ideal triangulation of $\mathbb{S}^3 \setminus (L \cup \{\text{two points}\})$, and name it *five-term triangulation*. (We rename the octahedral triangulation in [1] *four-term triangulation*. Both five-term and four-term triangulations use the same octahedral decomposition, but the ways of subdividing it into tetrahedra are different.) The two points are denoted by $\pm\infty$. Then we consider (Thurston's) gluing equations and the completeness condition of the five-term triangulation. (See Section 3 for exact definitions of these conditions.) These two conditions are expressed by equations of shape parameters and we call them *hyperbolicity equations*. One of the most important properties of the potential function W is the following proposition.

Proposition 1.1. *For a hyperbolic link L with a fixed diagram, consider the potential function $W(w_1, \dots, w_n)$ of the diagram. Then the set \mathcal{I} defined in (1) becomes the hyperbolicity equations of the five-term triangulation of $\mathbb{S}^3 \setminus (L \cup \{\pm\infty\})$.*

We remark that Proposition 1.1 was already proved in [2]. Therefore, we will sketch the proof in Section 3.

Let $\mathcal{T} = \{(w_1, \dots, w_n)\}$ be the set of solutions¹ of \mathcal{I} in \mathbb{C}^n . In this article, we always assume $\mathcal{T} \neq \emptyset$. Then, by Theorem 1 of [10], all edges in the five-term triangulation are essential. (Essential edge roughly means it is not null-homotopic. See [10] for the exact definition.) Therefore, using Yoshida's construction in Section 4.5 of [6], for a solution $\mathbf{w} \in \mathcal{T}$, we can construct a boundary-parabolic representation²

$$\rho_{\mathbf{w}} : \pi_1(\mathbb{S}^3 \setminus (L \cup \{\pm\infty\})) = \pi_1(\mathbb{S}^3 \setminus L) \longrightarrow \mathrm{PSL}(2, \mathbb{C}). \quad (2)$$

Note that the volume $\mathrm{vol}(\rho_{\mathbf{w}})$ and the Chern-Simons invariant $\mathrm{cs}(\rho_{\mathbf{w}})$ of $\rho_{\mathbf{w}}$ were defined in [12]. We call $\mathrm{vol}(\rho_{\mathbf{w}}) + i \mathrm{cs}(\rho_{\mathbf{w}})$ the *complex volume* of $\rho_{\mathbf{w}}$.

¹ We only consider solutions satisfying the condition that, when the potential function is expressed by $W(w_1, \dots, w_n) = \sum \pm \mathrm{Li}_2(w) + (\text{extra terms})$, the variables inside the dilogarithms satisfy $w \notin \{0, 1, \infty\}$. Previously, in [11] and [2], these solutions were called *essential solutions*.

² The solution $\mathbf{w} \in \mathcal{T}$ satisfies the completeness condition, so $\rho_{\mathbf{w}}$ is boundary-parabolic.

For the solution set $\mathcal{T} \subset \mathbb{C}^n$, let \mathcal{T}_j be a path component of \mathcal{T} satisfying $\mathcal{T} = \cup_{j \in J} \mathcal{T}_j$ for some index set J . We assume $0 \in J$ for notational convenience. To obtain well-defined values from the potential function $W(w_1, \dots, w_n)$, we slightly modify it to

$$W_0(w_1, \dots, w_n) := W(w_1, \dots, w_n) - \sum_{k=1}^n \left(w_k \frac{\partial W}{\partial w_k} \right) \log w_k. \quad (3)$$

Then the main result of this article follows.

Theorem 1.2. *Let L be a hyperbolic link with a fixed diagram and $W(w_1, \dots, w_n)$ be the potential function of the diagram. Assume the solution set $\mathcal{T} = \cup_{j \in J} \mathcal{T}_j$ is not empty. Then, for any $\mathbf{w} \in \mathcal{T}_j$, $W_0(\mathbf{w})$ is constant (depends only on j) and*

$$W_0(\mathbf{w}) \equiv i(\text{vol}(\rho_{\mathbf{w}}) + i \text{cs}(\rho_{\mathbf{w}})) \pmod{\pi^2}, \quad (4)$$

where $\rho_{\mathbf{w}}$ is the boundary-parabolic representation obtained in (2). Furthermore, there exists a path component \mathcal{T}_0 of \mathcal{T} satisfying

$$W_0(\mathbf{w}_{\infty}) \equiv i(\text{vol}(L) + i \text{cs}(L)) \pmod{\pi^2}, \quad (5)$$

for all $\mathbf{w}_{\infty} \in \mathcal{T}_0$.

The proof will be given in Section 4. The main idea is to use Zickert's formula of the extended Bloch group in [12]. Although the idea was already used in [1] and several other places, this proof had not appeared anywhere before.

We call the value $W_0(\mathbf{w})$ the *optimistic limit of the colored Jones polynomial*. Note that it depends on the choice of the diagram and the path component \mathcal{T}_j .

In Section 5, we will survey the results of [2]. In short, we define another potential function $V(z_1, \dots, z_g)$ from the diagram D of the hyperbolic link L and consider the set of equations

$$\mathcal{H} := \left\{ \exp \left(z_k \frac{\partial V}{\partial z_k} \right) = 1 \mid k = 1, \dots, g \right\}.$$

Then the set \mathcal{H} becomes the hyperbolicity equations of the four-term triangulation of $\mathbb{S}^3 \setminus (L \cup \{\pm\infty\})$. Let $\mathcal{S} = \{(z_1, \dots, z_g)\}$ be the set of solutions of \mathcal{H} in \mathbb{C}^g . Then, for a solution $\mathbf{z} \in \mathcal{S}$, we can obtain a boundary-parabolic representation

$$\rho_{\mathbf{z}} : \pi_1(\mathbb{S}^3 \setminus (L \cup \{\pm\infty\})) = \pi_1(\mathbb{S}^3 \setminus L) \longrightarrow \text{PSL}(2, \mathbb{C}).$$

Now we modify the potential function V to

$$V_0(z_1, \dots, z_g) := V(z_1, \dots, z_g) - \sum_{k=1}^g \left(z_k \frac{\partial V}{\partial z_k} \right) \log z_k.$$

Then the main result of [2] can be summarized to the following identity:

$$V_0(\mathbf{z}) \equiv i(\text{vol}(\rho_{\mathbf{z}}) + i \text{cs}(\rho_{\mathbf{z}})) \pmod{\pi^2}. \quad (6)$$

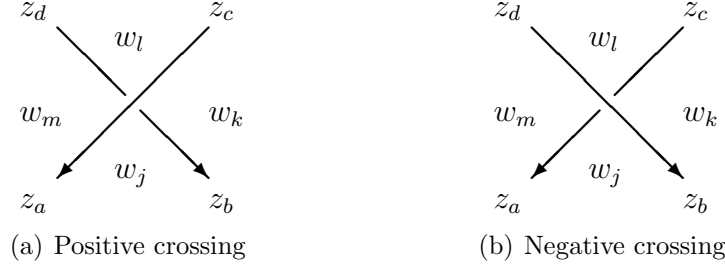


Figure 1: Assignment of variables

Note that the variables w_1, \dots, w_n and z_1, \dots, z_g are assigned to regions and sides of the diagram D respectively. (See Figure 1.) Combining the results of (4) and (6), we can easily see that, if $\rho_{\mathbf{w}} = \rho_{\mathbf{z}}$, then

$$W_0(\mathbf{w}) \equiv V_0(\mathbf{z}) \pmod{\pi^2}. \quad (7)$$

On the other hand, we can obtain much stronger relation than (7) as follows.

Theorem 1.3. *Assume the diagram D of the hyperbolic link L does not have a kink. For a solution $\mathbf{w} \in \mathcal{T}$, if the variables w_j, \dots, w_m in Figure 1 satisfy*

$$w_j + w_l \neq w_k + w_m$$

at all crossings, then there exists a solution $\mathbf{z} \in \mathcal{S}$ satisfying

$$\rho_{\mathbf{w}} = \rho_{\mathbf{z}} \text{ and } W_0(\mathbf{w}) \equiv V_0(\mathbf{z}) \pmod{4\pi^2}. \quad (8)$$

Inversely, for a solution $\mathbf{z} \in \mathcal{S}$, if the variables z_a, \dots, z_d in Figure 1 satisfy

$$z_a \neq z_c \text{ and } z_b \neq z_d$$

at all crossings, then there exists a solution $\mathbf{w} \in \mathcal{T}$ satisfying (8).

The proof of Theorem 1.3 was essentially appeared in [2], so we will sketch the proof in Section 6.

Finally, in Section 7, we will apply Theorem 1.3 to the example of twist knots and show several numerical calculations.

2 Potential function $W(w_1, \dots, w_n)$

Consider a hyperbolic link L and its oriented diagram D . We define *sides* of D by the arcs connecting two adjacent crossing points.³ For example, the diagram of the figure-eight knot 4_1 in Figure 2 has 8 sides. Also we define *regions* of D by regions surrounded by sides. For example, the diagram in Figure 2 has 6 regions.

³ Most people use the word *edge* instead of *side* here. However, in this paper, we want to keep the word *edge* for the edge of a tetrahedron.

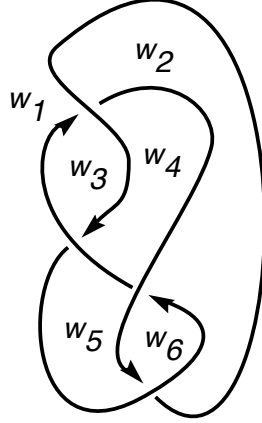


Figure 2: The figure-eight knot 4_1

We assign complex variables w_1, \dots, w_n to each region of the diagram D . Using the dilogarithm function $\text{Li}_2(w) = -\int_0^w \frac{\log(1-t)}{t} dt$, we define the potential function⁴ of a crossing as in Figure 3.

$$\begin{array}{c} \nearrow w_l \\ \nwarrow w_m \end{array} \begin{array}{c} \nearrow w_k \\ \nwarrow w_j \end{array} \longrightarrow W_P := -\text{Li}_2\left(\frac{w_l}{w_m}\right) - \text{Li}_2\left(\frac{w_l}{w_k}\right) + \text{Li}_2\left(\frac{w_j w_l}{w_k w_m}\right) + \text{Li}_2\left(\frac{w_m}{w_j}\right) + \text{Li}_2\left(\frac{w_k}{w_j}\right) - \frac{\pi^2}{6} + \log \frac{w_m}{w_j} \log \frac{w_k}{w_j}$$

(a) Positive crossing

$$\begin{array}{c} \nearrow w_l \\ \nwarrow w_m \end{array} \begin{array}{c} \nwarrow w_k \\ \nearrow w_j \end{array} \longrightarrow W_N := \text{Li}_2\left(\frac{w_l}{w_m}\right) + \text{Li}_2\left(\frac{w_l}{w_k}\right) - \text{Li}_2\left(\frac{w_j w_l}{w_k w_m}\right) - \text{Li}_2\left(\frac{w_m}{w_j}\right) - \text{Li}_2\left(\frac{w_k}{w_j}\right) + \frac{\pi^2}{6} - \log \frac{w_m}{w_j} \log \frac{w_k}{w_j}$$

(b) Negative crossing

Figure 3: Potential functions of the crossings

Note that this potential function comes from the formal substitution of the R-matrix of the colored Jones polynomial. Refer [2] for details.

⁴ Note that, by using the notation in Lemma 3.1 of [2], we know

$$\log \frac{w_j}{w_m} \log \frac{w_j}{w_k} \approx (\log w_j - \log w_m)(\log w_j - \log w_k) \approx \log \frac{w_m}{w_j} \log \frac{w_k}{w_j}.$$

Therefore, changing $\log \frac{w_j}{w_m} \log \frac{w_j}{w_k}$ of W_N to $\log \frac{w_m}{w_j} \log \frac{w_k}{w_j}$ does not have any effect on \mathcal{I} and the optimistic limit. To avoid redundant calculation, we will use $\log \frac{w_j}{w_m} \log \frac{w_j}{w_k}$ up to Section 4 and change it to $\log \frac{w_m}{w_j} \log \frac{w_k}{w_j}$ in Section 6.

The potential function $W(w_1, \dots, w_n)$ of the diagram D is defined by the summation of all potential functions of the crossings. For example, the potential function of the figure-eight knot 4_1 in Figure 2 is

$$\begin{aligned}
W(w_1, \dots, w_6) &= \left\{ -\text{Li}_2\left(\frac{w_1}{w_3}\right) - \text{Li}_2\left(\frac{w_1}{w_2}\right) + \text{Li}_2\left(\frac{w_1 w_4}{w_2 w_3}\right) + \text{Li}_2\left(\frac{w_3}{w_4}\right) + \text{Li}_2\left(\frac{w_2}{w_4}\right) - \frac{\pi^2}{6} + \log \frac{w_3}{w_4} \log \frac{w_2}{w_4} \right\} \\
&+ \left\{ -\text{Li}_2\left(\frac{w_4}{w_3}\right) - \text{Li}_2\left(\frac{w_4}{w_5}\right) + \text{Li}_2\left(\frac{w_1 w_4}{w_3 w_5}\right) + \text{Li}_2\left(\frac{w_3}{w_1}\right) + \text{Li}_2\left(\frac{w_5}{w_1}\right) - \frac{\pi^2}{6} + \log \frac{w_3}{w_1} \log \frac{w_5}{w_1} \right\} \\
&+ \left\{ \text{Li}_2\left(\frac{w_2}{w_4}\right) + \text{Li}_2\left(\frac{w_2}{w_6}\right) - \text{Li}_2\left(\frac{w_2 w_5}{w_4 w_6}\right) - \text{Li}_2\left(\frac{w_4}{w_5}\right) - \text{Li}_2\left(\frac{w_6}{w_5}\right) + \frac{\pi^2}{6} - \log \frac{w_4}{w_5} \log \frac{w_6}{w_5} \right\} \\
&+ \left\{ \text{Li}_2\left(\frac{w_5}{w_1}\right) + \text{Li}_2\left(\frac{w_5}{w_6}\right) - \text{Li}_2\left(\frac{w_2 w_5}{w_1 w_6}\right) - \text{Li}_2\left(\frac{w_1}{w_2}\right) - \text{Li}_2\left(\frac{w_6}{w_2}\right) + \frac{\pi^2}{6} - \log \frac{w_1}{w_2} \log \frac{w_6}{w_2} \right\}.
\end{aligned}$$

We define a modified potential function $W_0(w_1, \dots, w_n)$ as in (3). Recall that \mathcal{I} was defined in (1). Also recall that we are considering the solutions $\mathbf{w} = (w_1, \dots, w_n) \in \mathbb{C}^n$ of \mathcal{I} with the property that if the potential function is expressed by $W(w_1, \dots, w_n) = \sum \pm \text{Li}_2(w) +$ (extra terms), then variables inside the dilogarithms satisfy $w \notin \{0, 1, \infty\}$. In this article, we always assume the solution set $\mathcal{T} \subset \mathbb{C}^n$ of \mathcal{I} is nonempty.

Note that the functions $\text{Li}_2(w)$ and $\log w$ are multi-valued functions. Therefore, to obtain well-defined values, we have to select proper branch of the logarithm by choosing $\arg w$ and $\arg(1 - w)$. The following lemma, which corresponds to Lemma 2.1 of [1], shows why we consider the potential function W_0 instead of W .

Lemma 2.1. *Let $\mathbf{w} = (w_1, \dots, w_n) \in \mathcal{T}$. For the potential function $W(w_1, \dots, w_n)$, the value of $W_0(\mathbf{w})$ is invariant under any choice of branch of the logarithm modulo $4\pi^2$.*

Proof. Note that it was almost proved in Lemma 2.1 of [1]. Using the idea in [1], we can write down

$$W_0^*(\mathbf{w}) - W_0(\mathbf{w}) \equiv \sum_{k=1}^n \left\{ - \left(w_k \frac{\partial W}{\partial w_k} \right) \log^* w_k + \left(w_k \frac{\partial W}{\partial w_k} \right) \log w_k \right\} \pmod{4\pi^2}, \quad (9)$$

where $W^*(\mathbf{w})$ and $\log^* w$ are the functions with different log-branch corresponding to an analytic continuation of $W(\mathbf{w})$ and $\log w$ respectively. We already assumed $\mathbf{w} = (w_1, \dots, w_n) \in \mathcal{T}$, so we obtain

$$\left(w_k \frac{\partial W}{\partial w_k} \right) \log^* w_k \equiv \left(w_k \frac{\partial W}{\partial w_k} \right) \log w_k \pmod{4\pi^2},$$

and (9) is zero modulo $4\pi^2$. □

The following lemma and corollary were already appeared and proved in [1] as Lemma 2.2 and Corollary 2.3 respectively. Hence, we skip the proofs here.

Lemma 2.2. Let $\mathcal{T} = \cup_{j \in J} \mathcal{T}_j \subset \mathbb{C}^n$ be the solution set of \mathcal{I} with \mathcal{T}_j being a path component. Assume $\mathcal{T} \neq \emptyset$. Then, for any $\mathbf{w} = (w_1, \dots, w_n) \in \mathcal{T}_j$,

$$W_0(\mathbf{w}) \equiv C_j \pmod{4\pi^2},$$

where C_j is a complex constant depending only on $j \in J$.

Corollary 2.3. If $\mathbf{w} = (w_1, \dots, w_n) \in \mathcal{T}_j$, then

$$\lambda \mathbf{w} := (\lambda w_1, \dots, \lambda w_n) \in \mathcal{T}_j$$

for any nonzero complex number λ . Furthermore,

$$W_0(\mathbf{w}) \equiv W_0(\lambda \mathbf{w}) \pmod{4\pi^2}.$$

Due to Corollary 2.3, we can consider the solution set \mathcal{T} as a subset of \mathbb{CP}^{n-1} instead of \mathbb{C}^n .

3 Five-term triangulation of $\mathbb{S}^3 \setminus (L \cup \{\pm\infty\})$

In this section, we describe the five-term triangulation of $\mathbb{S}^3 \setminus (L \cup \{\text{two points}\})$. We remark that this triangulation was previously named Thurston triangulation in [2].

We place an octahedron $A_r B_r C_r D_r E_r F_r$ on each crossing r of the link diagram as in Figure 4 so that the vertices A_r and C_r lie on the over-bridge and the vertices B_r and D_r on the under-bridge of the diagram respectively. Then we twist the octahedron by gluing edges $B_r F_r$ to $D_r F_r$ and $A_r E_r$ to $C_r E_r$ respectively. The edges $A_r B_r$, $B_r C_r$, $C_r D_r$ and $D_r A_r$ are called *horizontal edges* and we sometimes express these edges in the diagram as arcs around the crossing in the left-hand side of Figure 4.

Then we glue faces of the octahedra following the sides of the diagram. Specifically, there are three gluing patterns as in Figure 5. In each cases (a), (b) and (c), we identify the faces $\triangle A_r B_r E_r \cup \triangle C_r B_r E_r$ to $\triangle C_{r+1} D_{r+1} F_{r+1} \cup \triangle C_{r+1} B_{r+1} F_{r+1}$, $\triangle B_r C_r F_r \cup \triangle D_r C_r F_r$ to $\triangle D_{r+1} C_{r+1} F_{r+1} \cup \triangle B_{r+1} C_{r+1} F_{r+1}$ and $\triangle A_r B_r E_r \cup \triangle C_r B_r E_r$ to $\triangle C_{r+1} B_{r+1} E_{r+1} \cup \triangle A_{r+1} B_{r+1} E_{r+1}$ respectively. We call (a) *alternating gluing*, (b) and (c) *non-alternating gluings*.

Note that this gluing process identifies vertices $\{A_r, C_r\}$ to one point, denoted by $-\infty$, and $\{B_r, D_r\}$ to another point, denoted by ∞ , and finally $\{E_r, F_r\}$ to the other points, denoted by P_j where $j = 1, \dots, s$ and s is the number of the components of the link L . The regular neighborhoods of $-\infty$ and ∞ are 3-balls and that of $\cup_{j=1}^s P_j$ is a tubular neighborhood of the link L . Therefore, if we remove the vertices P_1, \dots, P_s from the tetrahedra, then we obtain a decomposition of $\mathbb{S}^3 \setminus L$, denoted by T . On the other hand, if we remove all the vertices of the tetrahedra, the result becomes an ideal decomposition of $\mathbb{S}^3 \setminus (L \cup \{\pm\infty\})$. We call the latter *the octahedral decomposition* and denote it by T' .

To obtain an ideal triangulation from T' , we divide each octahedron $A_r B_r C_r D_r E_r F_r$ in Figure 4 into five ideal tetrahedra $A_r B_r D_r F_r$, $B_r C_r D_r F_r$, $A_r B_r C_r D_r$, $A_r B_r C_r E_r$ and $A_r C_r D_r E_r$. We call the result *the five-term triangulation* of $\mathbb{S}^3 \setminus (L \cup \{\pm\infty\})$. On the other hand, if we

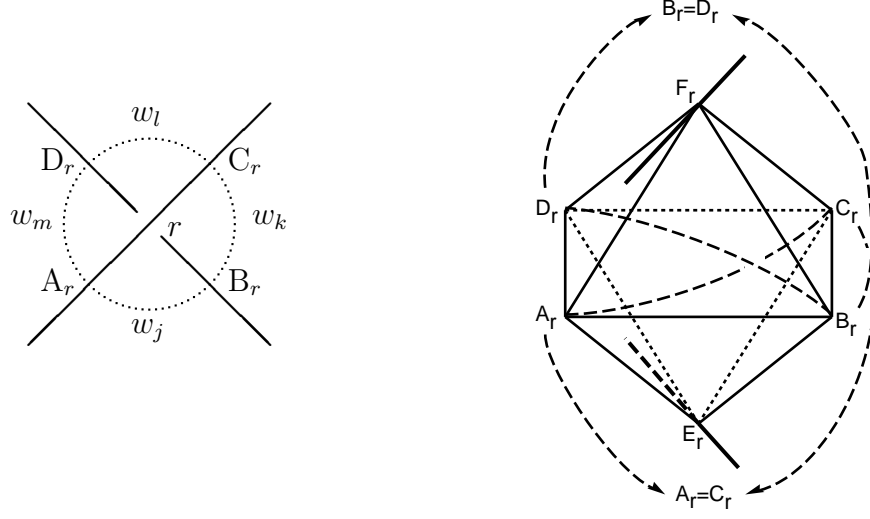


Figure 4: Octahedron on the crossing r

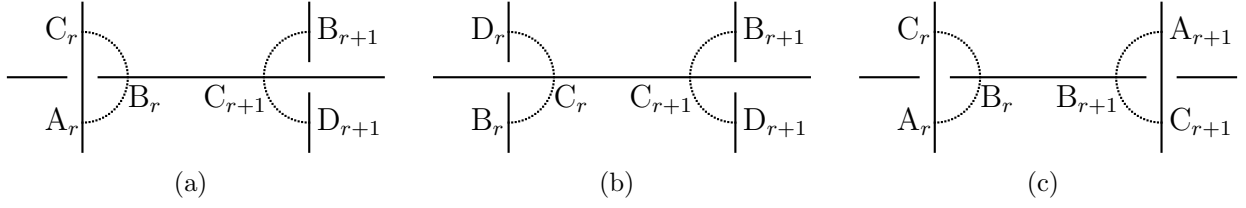


Figure 5: Three gluing patterns

divide the same octahedron into four ideal tetrahedra $A_r B_r E_r F_r$, $B_r C_r E_r F_r$, $C_r D_r E_r F_r$ and $D_r A_r E_r F_r$, then the result is called *the four-term triangulation*. The four-term triangulation was used in [1] and will appear again in Section 5 and Section 6 of this article.

Note that if we assign the shape parameter $u \in \mathbb{C} \setminus \{0, 1\}$ to an edge of an ideal hyperbolic tetrahedron, then the other edges are also parametrized by $u, u' := \frac{1}{1-u}$ and $u'' := 1 - \frac{1}{u}$ as in Figure 6.

To determine the shape of the octahedron in Figure 4, we assign shape parameters to edges of tetrahedra as in Figure 7. Note that both of $\frac{w_j w_l}{w_k w_m}$ in Figure 7(a) and $\frac{w_k w_m}{w_j w_l}$ in Figure 7(b) are the shape parameters of the tetrahedron $A_r B_r C_r D_r$ assigned to the edges $B_r D_r$ and $A_r C_r$. Also note that the assignment of shape parameters here does not depend on the orientations of the link diagram.

To obtain the boundary parabolic representation $\pi_1(\mathbb{S}^3 \setminus (L \cup \{\pm\infty\})) \rightarrow \text{PSL}(2, \mathbb{C})$, we require two conditions on the ideal triangulation of $\mathbb{S}^3 \setminus (L \cup \{\pm\infty\})$; the product of shape parameters on any edge in the triangulation becomes one, and the holonomies induced by meridian and longitude of the torus cusps act as translations on the torus cusp. Note that these conditions are expressed as equations of shape parameters. The former equations

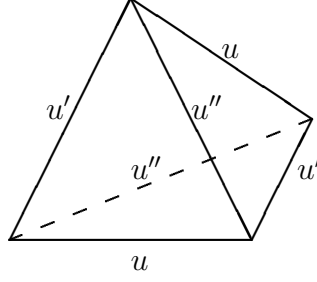


Figure 6: Parametrization of an ideal tetrahedron with a shape parameter u

are called (*Thurston's*) *gluing equations*, the latter is called *completeness condition*, and the whole set of these equations are called *the hyperbolicity equations*. As already discussed in [1] and Section 1, a solution \mathbf{w} of the hyperbolicity equation determines a boundary-parabolic representation

$$\rho_{\mathbf{w}} : \pi_1(\mathbb{S}^3 \setminus (L \cup \{\pm\infty\})) = \pi_1(\mathbb{S}^3 \setminus L) \longrightarrow \mathrm{PSL}(2, \mathbb{C}).$$

The rest of this section is devoted to the proof of Proposition 1.1. It was already proved⁵ in [2], so we sketch the proof here.

Sketch of the proof of Proposition 1.1. For all the crossings of the link diagram and the corresponding octahedra in Figure 4, let \mathcal{A} be the set of horizontal edges $A_r B_r$, $B_r C_r$, $C_r D_r$ and $D_r A_r$. Let \mathcal{B} be the set of edges $B_r F_r$, $D_r F_r$, $A_r E_r$, $C_r E_r$ of all crossings and other edges glued to them. Let \mathcal{C} be the set of edges $A_r C_r$ and $B_r D_r$ of all crossings. Finally, let \mathcal{D} be the set of all the other edges in the triangulation. Note that if the link diagram is alternating, then $\mathcal{D} = \emptyset$.

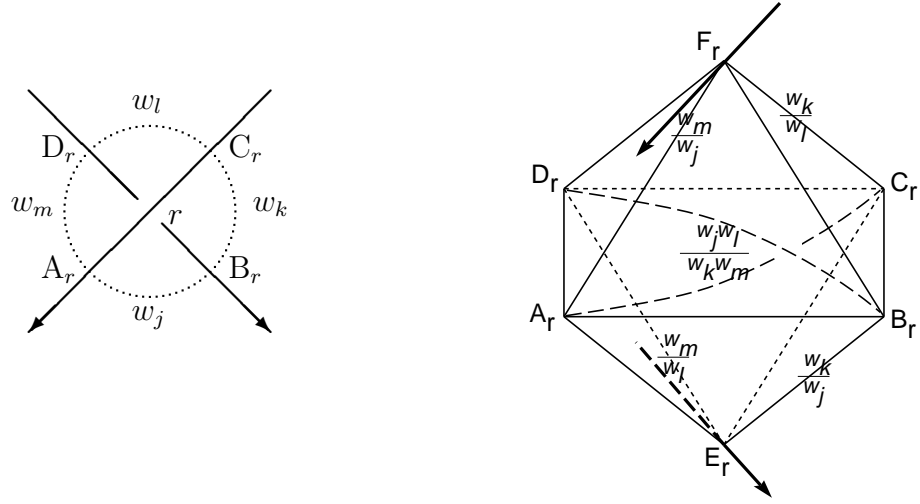
Direct calculation shows that $\exp(w_a \frac{\partial W_P}{\partial w_a})$ for $a = j, k, l, m$ is the product of the shape parameters assigned to the horizontal edge corresponding to the region w_a in Figure 7(a). For example,

$$\exp\left(w_j \frac{\partial W_P}{\partial w_j}\right) = \left(\frac{w_j w_l}{w_k w_m}\right)' \left(\frac{w_m}{w_j}\right)'' \left(\frac{w_k}{w_j}\right)'' ,$$

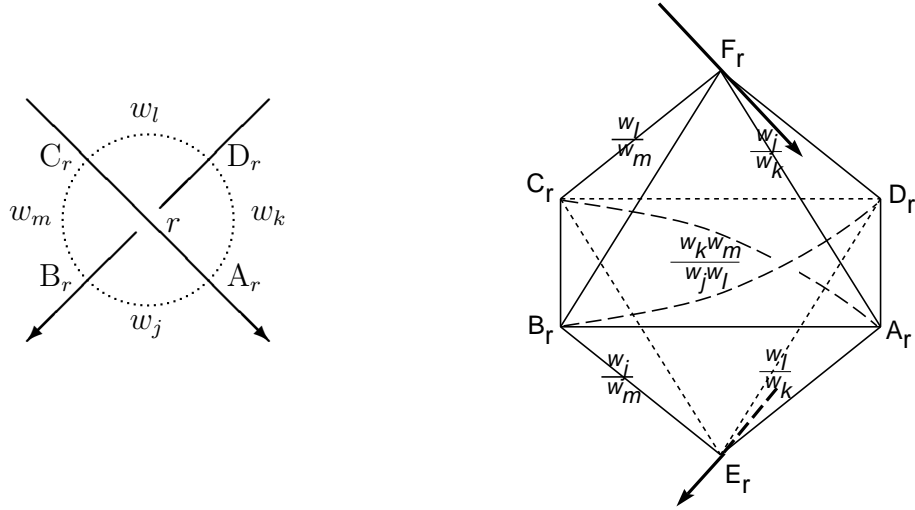
which is the product of the shape parameters assigned to the edge $A_r B_r$. (See (8)–(10) of [2] for the other equations. In [2], our W_P and W_N were denoted by P_1 and N_1 respectively.) Furthermore, the same holds for $\exp(w_a \frac{\partial W_N}{\partial w_a})$ too. Therefore, \mathcal{I} becomes the gluing equations of the edges in \mathcal{A} .

The gluing equations of the edges in \mathcal{C} and \mathcal{D} hold trivially because of the assigning rule of the shape parameters to the tetrahedra. We will show that the gluing equations of the edges in \mathcal{B} hold trivially too. Consider the alternating gluing in Figure 8(a). This induces a part of the cusp diagram as in Figure 8(b), which comes from the gluing of two tetrahedra

⁵ The proof is in Lemma 4.1 and Proposition 1.1 of [2], which started with the general case, and then proceeded to the collapsed cases. In this article, the collapsed cases do not happen, so the general case is enough.



(a) Positive crossing



(b) Negative crossing

Figure 7: Assignment of shape parameters

in Figure 8(c). On the other hand, the non-alternating gluings in Figure 5(b) and (c) do not have any effect on the cusp diagram of the torus cusp.

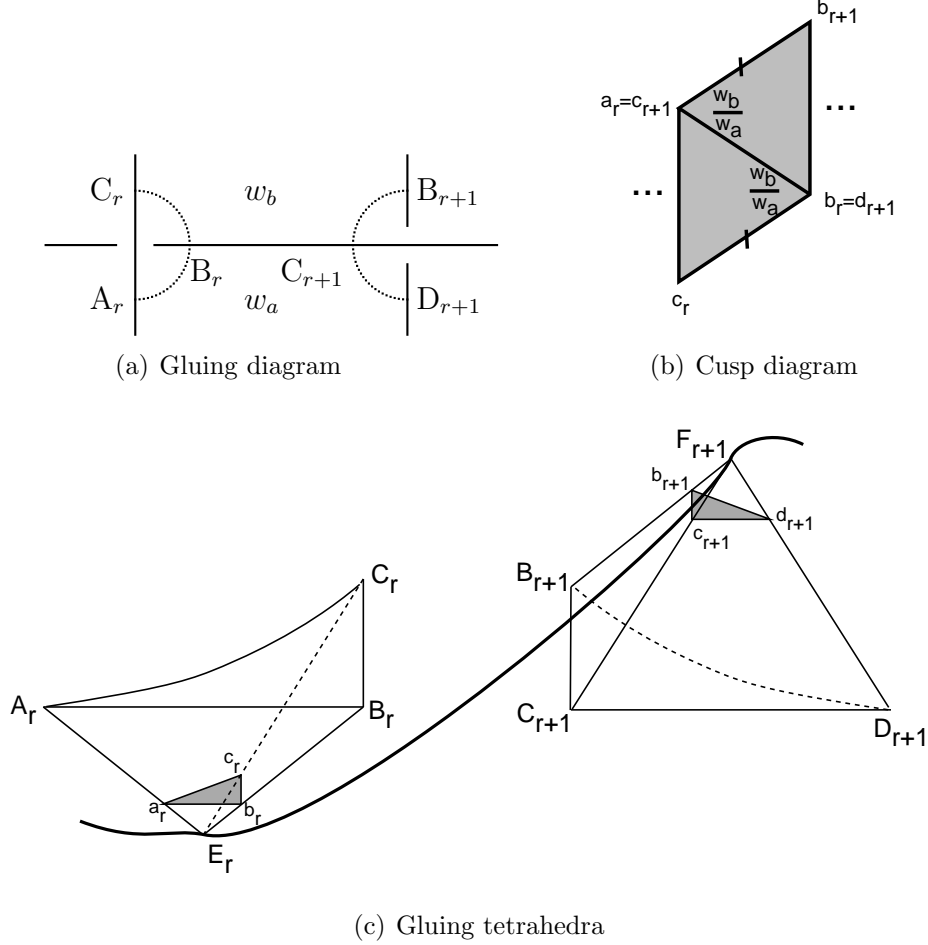


Figure 8: Cusp diagram induced from Figure 6(a)

Note that the cusp diagram in Figure 8(b) is an annulus because the edge $c_{r+1}b_{r+1}$ is identified with $c_r b_r$. The shape parameter $\frac{w_b}{w_a}$ is assigned to the edges $B_r E_r$ and $C_{r+1} F_{r+1}$ in Figure 8(c), and the product of shape parameters on the edge $B_r E_r = B_{r+1} F_{r+1} = D_{r+1} F_{r+1} \in \mathcal{B}$ (around the vertex $b_r = b_{r+1} = d_{r+1}$ in Figure 8(b)) is

$$\frac{w_b}{w_a} \left(\frac{w_b}{w_a} \right)'' \left(\frac{w_b}{w_a} \right)' = -1.$$

Therefore, if we consider another annulus on the right-hand side of the edge $b_{r+1} d_{r+1}$ in Figure 8(b), the gluing equation of the edge $B_r E_r = B_{r+1} F_{r+1} = D_{r+1} F_{r+1} \in \mathcal{B}$ is satisfied trivially.

The other gluing equations of the edges in \mathcal{B} can be obtained in the same way. Hence, we conclude \mathcal{I} induces the gluing equations of all the edges in $\mathcal{A} \cup \mathcal{B} \cup \mathcal{C} \cup \mathcal{D}$. Furthermore,

the cusp diagram in Figure 8(b) already satisfies one completeness condition of the meridian that sends the edge $c_r b_r$ to $c_{r+1} b_{r+1}$. Therefore, \mathcal{I} induces all the hyperbolicity equations. \square

4 Proof of Theorem 1.2

In this section, we always assume $\mathbf{w} = (w_1, \dots, w_n)$ is a solution in \mathcal{T} . The main technique of the proof of Theorem 1.2 is the extended Bloch group theory in [12]. To apply it, we first define the vertex ordering of the five-term triangulation in Figure 9 so that the order 0, 1, 2, 3 is assigned to the vertices of each tetrahedra in the order of $D_r B_r F_r A_r$, $B_r E_r A_r C_r$, $D_r B_r F_r C_r$, $D_r E_r A_r C_r$ and $D_r B_r A_r C_r$.

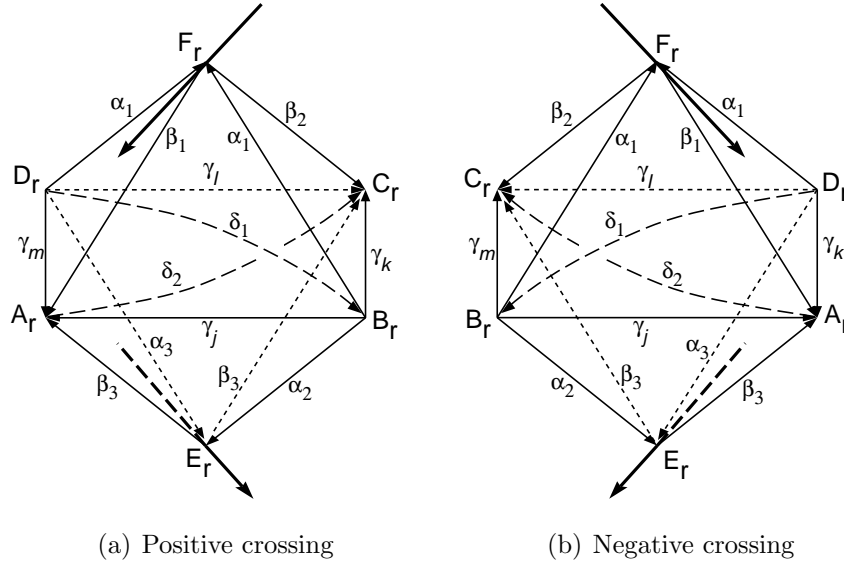


Figure 9: Vertex orderings and labelings of edges

Note that the vertex ordering of each tetrahedron induces the orientations of the edges and the tetrahedron. The induced orientation of the tetrahedron can be different from the original orientation induced by the triangulation. For example, the tetrahedra $D_r B_r F_r C_r$ and $D_r E_r A_r C_r$ in Figure 9(a), $D_r B_r F_r A_r$, $B_r E_r A_r C_r$ and $D_r B_r A_r C_r$ in Figure 9(b) are the cases. If the two orientations are the same, we define the sign of the tetrahedron $\sigma = 1$, and if they are different, then $\sigma = -1$.

One important property of our vertex orientation is that when two edges are glued together in the triangulation, the orientations of the two edges induced by each vertex orderings coincide. (We call this condition *edge-orientation consistency*.) Because of this property, we can apply the formula in [12].

The five-term triangulation we are using is an ideal triangulation, so we parametrized all ideal tetrahedra of the triangulation by assigning shape parameters as in Figure 7. For each tetrahedron with the vertex-orientation, we define an element of the extended pre-Bloch

group $\sigma[u^\sigma; p, q] \in \widehat{\mathcal{P}}(\mathbb{C})$, where σ is the sign of the tetrahedron, u is the shape parameter assigned to the edge connecting the 0th and 1st vertices, and p, q are certain integers.

Zickert suggested a way to determine p and q from the developing map of the representation $\rho : \pi_1(M) \rightarrow \text{PSL}(2, \mathbb{C})$ of a hyperbolic manifold M in [12], and showed that

$$\widehat{L}\left(\sum \sigma[u^\sigma; p, q]\right) \equiv i(\text{vol}(\rho) + i \text{cs}(\rho)) \pmod{\pi^2}, \quad (10)$$

where the summation is over all tetrahedra and

$$\widehat{L}([u; p, q]) = \text{Li}_2(u) - \frac{\pi^2}{6} + \frac{1}{2}q\pi i \log u + \frac{1}{2}(p\pi i + \log u) \log(1 - u)$$

is a complex valued function defined on $\widehat{\mathcal{P}}(\mathbb{C})$.

Although our five-term triangulation is for $\mathbb{S}^3 \setminus (L \cup \{\pm\infty\})$, the formula of [12] is still valid because of Thurston's spinning construction. (See [6] for Thurston's spinning construction and refer [1] for details.)

To determine p, q of $\sigma[u^\sigma; p, q]$ corresponding to each tetrahedron with vertex orientation, we assign certain complex numbers g_{jk} to the edge connecting the j th and k th vertices, where $j, k \in \{0, 1, 2, 3\}$ and $j < k$. We assume g_{jk} satisfies the property that if two edges are glued together in the triangulation, then the assigned g_{jk} 's of the glued edges coincide. We do not use the exact values of g_{jk} in this article, but remark that there is an explicit method in [12] for calculating these numbers using the developing map. With the given numbers g_{jk} , we can calculate p, q using the following equation, which appeared as equation (3.5) in [12]:

$$\begin{cases} p\pi i = -\log u^\sigma + \log g_{03} + \log g_{12} - \log g_{02} - \log g_{13}, \\ q\pi i = \log(1 - u^\sigma) + \log g_{02} + \log g_{13} - \log g_{01} - \log g_{23}. \end{cases} \quad (11)$$

To avoid confusion, we use variables $\alpha_1, \alpha_2, \alpha_3, \beta_1, \beta_2, \beta_3, \gamma_j, \gamma_k, \gamma_l, \gamma_m, \delta_1$ and δ_2 instead of g_{jk} as in Figure 9. Note that γ_a ($a = j, k, l, m$) is assigned to the horizontal edge that lies in the region with w_a . The orientation we defined in Figure 9 satisfies the edge-orientation consistency, so we will apply the formula of [12] to our five-term triangulation.

For the positive crossing r in Figure 9(a), let $\sigma_1^{(r)}[u_1^{\sigma_1^{(r)}}; p_1^{(r)}, q_1^{(r)}], \dots, \sigma_5^{(r)}[u_5^{\sigma_5^{(r)}}; p_5^{(r)}, q_5^{(r)}]$ be the elements in $\widehat{\mathcal{P}}(\mathbb{C})$ corresponding to $D_r B_r F_r A_r, B_r E_r A_r C_r, D_r B_r F_r C_r, D_r E_r A_r C_r$ and $D_r B_r A_r C_r$ respectively. Then we have

$$\begin{aligned} \sigma_1^{(r)} &= \sigma_2^{(r)} = \sigma_5^{(r)} = 1, \quad \sigma_3^{(r)} = \sigma_4^{(r)} = -1, \\ u_1^{\sigma_1^{(r)}} &= \frac{w_m}{w_j}, \quad u_2^{\sigma_2^{(r)}} = \frac{w_k}{w_j}, \quad u_3^{\sigma_3^{(r)}} = \frac{w_l}{w_k}, \quad u_4^{\sigma_4^{(r)}} = \frac{w_l}{w_m}, \quad u_5^{\sigma_5^{(r)}} = \frac{w_j w_l}{w_k w_m}, \end{aligned}$$

and direct calculation from (11) shows

$$\begin{cases} p_1^{(r)}\pi i + \log \frac{w_m}{w_j} = \log \gamma_m - \log \gamma_j, \\ p_2^{(r)}\pi i + \log \frac{w_k}{w_j} = \log \gamma_k - \log \gamma_j, \\ p_3^{(r)}\pi i + \log \frac{w_l}{w_k} = \log \gamma_l - \log \gamma_k, \\ p_4^{(r)}\pi i + \log \frac{w_l}{w_m} = \log \gamma_l - \log \gamma_m, \\ p_5^{(r)}\pi i + \log \frac{w_j w_l}{w_k w_m} = \log \gamma_j + \log \gamma_l - \log \gamma_k - \log \gamma_m, \end{cases} \quad (12)$$

and

$$\begin{cases} q_1^{(r)} \pi i - \log(1 - \frac{w_m}{w_j}) = \log \alpha_1 + \log \gamma_j - \log \delta_1 - \log \beta_1, \\ q_2^{(r)} \pi i - \log(1 - \frac{w_k}{w_j}) = \log \gamma_j + \log \beta_3 - \log \alpha_2 - \log \delta_2, \\ q_3^{(r)} \pi i - \log(1 - \frac{w_l}{w_k}) = \log \alpha_1 + \log \gamma_k - \log \delta_1 - \log \beta_2, \\ q_4^{(r)} \pi i - \log(1 - \frac{w_l}{w_m}) = \log \gamma_m + \log \beta_3 - \log \alpha_3 - \log \delta_2, \\ q_5^{(r)} \pi i - \log(1 - \frac{w_j w_l}{w_k w_m}) = \log \gamma_m + \log \gamma_k - \log \delta_1 - \log \delta_2. \end{cases} \quad (13)$$

For the negative crossing r in Figure 9(b), let $\sigma_1^{(r)}[u_1^{\sigma_1^{(r)}}; p_1^{(r)}, q_1^{(r)}], \dots, \sigma_5^{(r)}[u_5^{\sigma_5^{(r)}}; p_5^{(r)}, q_5^{(r)}]$ be the elements in $\widehat{\mathcal{P}}(\mathbb{C})$ corresponding to $B_r E_r A_r C_r$, $D_r B_r F_r A_r$, $D_r E_r A_r C_r$, $D_r B_r F_r C_r$ and $D_r B_r A_r C_r$ respectively. Then we have

$$\sigma_1^{(r)} = \sigma_2^{(r)} = \sigma_5^{(r)} = -1, \quad \sigma_3^{(r)} = \sigma_4^{(r)} = 1, \\ u_1^{\sigma_1^{(r)}} = \frac{w_m}{w_j}, \quad u_2^{\sigma_2^{(r)}} = \frac{w_k}{w_j}, \quad u_3^{\sigma_3^{(r)}} = \frac{w_l}{w_k}, \quad u_4^{\sigma_4^{(r)}} = \frac{w_l}{w_m}, \quad u_5^{\sigma_5^{(r)}} = \frac{w_j w_l}{w_k w_m},$$

and direct calculation from (11) shows

$$\begin{cases} p_1^{(r)} \pi i + \log \frac{w_m}{w_j} = \log \gamma_m - \log \gamma_j, \\ p_2^{(r)} \pi i + \log \frac{w_k}{w_j} = \log \gamma_k - \log \gamma_j, \\ p_3^{(r)} \pi i + \log \frac{w_l}{w_k} = \log \gamma_l - \log \gamma_k, \\ p_4^{(r)} \pi i + \log \frac{w_l}{w_m} = \log \gamma_l - \log \gamma_m, \\ p_5^{(r)} \pi i + \log \frac{w_j w_l}{w_k w_m} = \log \gamma_j + \log \gamma_l - \log \gamma_k - \log \gamma_m, \end{cases} \quad (14)$$

and

$$\begin{cases} q_1^{(r)} \pi i - \log(1 - \frac{w_m}{w_j}) = \log \gamma_j + \log \beta_3 - \log \alpha_2 - \log \delta_2, \\ q_2^{(r)} \pi i - \log(1 - \frac{w_k}{w_j}) = \log \alpha_1 + \log \gamma_j - \log \delta_1 - \log \beta_1, \\ q_3^{(r)} \pi i - \log(1 - \frac{w_l}{w_k}) = \log \gamma_k + \log \beta_3 - \log \alpha_3 - \log \delta_2, \\ q_4^{(r)} \pi i - \log(1 - \frac{w_l}{w_m}) = \log \alpha_1 + \log \gamma_m - \log \delta_1 - \log \beta_2, \\ q_5^{(r)} \pi i - \log(1 - \frac{w_j w_l}{w_k w_m}) = \log \gamma_k + \log \gamma_m - \log \delta_1 - \log \delta_2. \end{cases} \quad (15)$$

From the above definitions, we can conclude

$$\sum_{r: \text{crossings}} \sum_{c=1}^5 \sigma_c^{(r)}[u_c^{\sigma_c^{(r)}}; p_c^{(r)}, q_c^{(r)}] \in \widehat{\mathcal{P}}(\mathbb{C})$$

is the corresponding element of the five-term triangulation. The following observation can be easily obtained.

Observation 4.1. *There exists a constant C satisfying*

$$\log w_b \equiv \log \gamma_b + C \pmod{\pi i},$$

for all $b = 1, \dots, n$.

Proof. The relation (12) or (14) holds for any crossing r of the link diagram. Therefore, by letting $C = \log w_1 - \log \gamma_1$, it follows trivially. \square

Now we define integer $Q_a^{(r)}$ for the crossing r and $a = j, k, l, m$ by the following ways. For the positive crossing r in Figure 9(a), we define

$$\begin{cases} Q_j^{(r)} = q_1^{(r)} + q_2^{(r)} - q_5^{(r)} + p_1^{(r)} + p_2^{(r)}, \\ Q_k^{(r)} = -q_2^{(r)} - q_3^{(r)} + q_5^{(r)} - p_1^{(r)}, \\ Q_l^{(r)} = q_3^{(r)} + q_4^{(r)} - q_5^{(r)}, \\ Q_m^{(r)} = -q_4^{(r)} - q_1^{(r)} + q_5^{(r)} - p_2^{(r)}, \end{cases} \quad (16)$$

and, for the negative crossing r in Figure 9(b), we define

$$\begin{cases} Q_j^{(r)} = -q_1^{(r)} - q_2^{(r)} + q_5^{(r)} - p_1^{(r)} - p_2^{(r)}, \\ Q_k^{(r)} = q_2^{(r)} + q_3^{(r)} - q_5^{(r)} + p_1^{(r)}, \\ Q_l^{(r)} = -q_3^{(r)} - q_4^{(r)} + q_5^{(r)}, \\ Q_m^{(r)} = q_4^{(r)} + q_1^{(r)} - q_5^{(r)} + p_2^{(r)}. \end{cases} \quad (17)$$

Note that, from the definitions (16) and (17), we can directly obtain

$$\sum_{a=j,k,l,m} Q_a^{(r)} = 0, \quad (18)$$

for any crossing r .

Lemma 4.2. *For the potential function $W(w_1, \dots, w_n)$ and the index $b = 1, \dots, n$, we have*

$$w_b \frac{\partial W}{\partial w_b} = \sum_r Q_b^{(r)} \pi i,$$

where r is over the crossings that lie on the boundary of the region associated with w_b .

Proof. Note that W_P and W_N were defined in Figure 3.

For the positive crossing r in Figure 9(a), direct calculation from (12) and (13) shows

$$\begin{cases} w_j \frac{\partial W_P}{\partial w_j} = Q_j^{(r)} \pi i + (\log \beta_1 - \log \alpha_1) + (\log \alpha_2 - \log \beta_3), \\ w_k \frac{\partial W_P}{\partial w_k} = Q_k^{(r)} \pi i + (\log \alpha_1 - \log \beta_2) + (\log \beta_3 - \log \alpha_2), \\ w_l \frac{\partial W_P}{\partial w_l} = Q_l^{(r)} \pi i + (\log \beta_2 - \log \alpha_1) + (\log \alpha_3 - \log \beta_3), \\ w_m \frac{\partial W_P}{\partial w_m} = Q_m^{(r)} \pi i + (\log \alpha_1 - \log \beta_1) + (\log \beta_3 - \log \alpha_3). \end{cases}$$

For the negative crossing r in Figure 9(b), direct calculation from (14) and (15) shows

$$\begin{cases} w_j \frac{\partial W_N}{\partial w_j} = Q_j^{(r)} \pi i + (\log \alpha_1 - \log \beta_1) + (\log \beta_3 - \log \alpha_2), \\ w_k \frac{\partial W_N}{\partial w_k} = Q_k^{(r)} \pi i + (\log \beta_1 - \log \alpha_1) + (\log \alpha_3 - \log \beta_3), \\ w_l \frac{\partial W_N}{\partial w_l} = Q_l^{(r)} \pi i + (\log \alpha_1 - \log \beta_2) + (\log \beta_3 - \log \alpha_3), \\ w_m \frac{\partial W_N}{\partial w_m} = Q_m^{(r)} \pi i + (\log \beta_2 - \log \alpha_1) + (\log \alpha_2 - \log \beta_3). \end{cases}$$

From the above calculations, we can find a general rule. Elaborating on $w_j \frac{\partial W_P}{\partial w_j}$, consider the faces $A_r B_r F_r$ and $A_r B_r E_r$ in Figure 9(a). The term $(\log \beta_1 - \log \alpha_1)$ in $w_j \frac{\partial W_P}{\partial w_j}$ comes from the edges $A_r F_r$ and $B_r F_r$ of the face $A_r B_r F_r$ counterclockwise, and the term $(\log \alpha_2 - \log \beta_3)$ comes from the edges $B_r E_r$ and $A_r E_r$ of the face $A_r B_r E_r$ clockwise. These rules hold for all the cases.

Consider the face $A_r B_r F_r$ and its corresponding term $(\log \beta_1 - \log \alpha_1)$. As in Figure 10, the face glued to $A_r B_r F_r$ induces the term $(\log \alpha_1 - \log \beta_1)$, which cancel out the term corresponding to $A_r B_r F_r$. (The shaded faces in Figure 10 are glued to $A_r B_r F_r$.) In the same way, all the other terms corresponding to the other faces are cancelled each other and the proof follows.

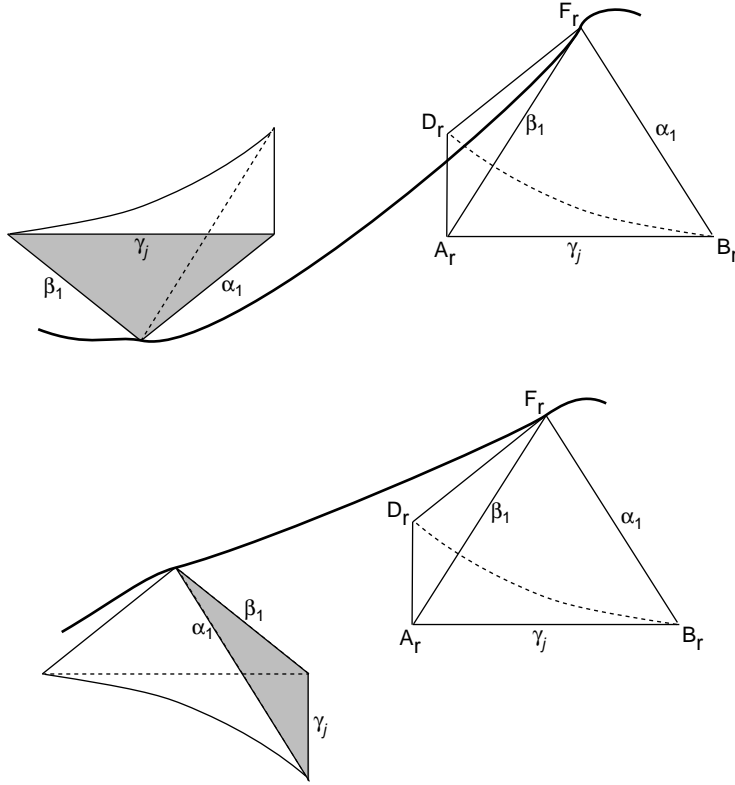


Figure 10: Two cases of the gluing of $A_r B_r F_r$

□

By combining (18) and Lemma 4.2, or by direct calculation, we have

$$\sum_{b=1}^n w_b \frac{\partial W}{\partial w_b} = 0. \quad (19)$$

To obtain (4), we need to use (10) and prove

$$W(w_1, \dots, w_n) - \sum_{b=1}^n \left(w_b \frac{\partial W}{\partial w_b} \right) \log w_b \equiv \widehat{L} \left(\sum_{r,c} \sigma_c^{(r)} [u_c^{\sigma_c^{(r)}}; p_c^{(r)}, q_c^{(r)}] \right) \pmod{\pi^2}, \quad (20)$$

where $c = 1, \dots, 5$ and r is over all crossings. At first, from (16) and (17), we have

$$\begin{aligned} \sum_{a=j,k,l,m} Q_a^{(r)} \pi i \log w_a &\equiv -\sigma_1^{(r)} \left\{ q_1^{(r)} \pi i \log \frac{w_m}{w_j} + q_2^{(r)} \pi i \log \frac{w_k}{w_j} - q_3^{(r)} \pi i \log \frac{w_l}{w_k} \right. \\ &\quad \left. - q_4^{(r)} \pi i \log \frac{w_l}{w_m} + q_5^{(r)} \pi i \log \frac{w_j w_l}{w_k w_m} + p_1^{(r)} \pi i \log \frac{w_k}{w_j} + p_2^{(r)} \pi i \log \frac{w_m}{w_j} \right\} \\ &\equiv - \sum_{c=1}^5 \sigma_c^{(r)} q_c^{(r)} \pi i \log u_c^{\sigma_c^{(r)}} - \sigma_1^{(r)} p_1^{(r)} \pi i \log u_2^{\sigma_2^{(r)}} - \sigma_1^{(r)} p_2^{(r)} \pi i \log u_1^{\sigma_1^{(r)}} \pmod{2\pi^2}. \end{aligned} \quad (21)$$

Combining (21) and Lemma 4.2, we obtain

$$\begin{aligned} \frac{1}{2} \sum_{r,c} \sigma_c^{(r)} q_c^{(r)} \pi i \log u_c^{\sigma_c^{(r)}} &\equiv -\frac{1}{2} \sum_{b=1}^n \left(w_b \frac{\partial W}{\partial w_b} \right) \log w_b \\ &\quad - \frac{1}{2} \sum_r \left\{ \sigma_1^{(r)} p_1^{(r)} \pi i \log u_2^{\sigma_2^{(r)}} + \sigma_1^{(r)} p_2^{(r)} \pi i \log u_1^{\sigma_1^{(r)}} \right\} \pmod{\pi^2}, \end{aligned} \quad (22)$$

where $c = 1, \dots, 5$ and r is over all crossings.

Let $W^{(r)}$ be the potential function of the crossing r , i.e.

$$W^{(r)} := \begin{cases} W_P & \text{if } r \text{ is a positive crossing,} \\ W_N & \text{if } r \text{ is a negative crossing.} \end{cases}$$

From (12), (14) and direct calculation, we obtain

$$\begin{aligned}
& \sum_{c=1}^5 \sigma_c^{(r)} (p_c^{(r)} \pi i + \log u_c^{\sigma_c^{(r)}}) \log(1 - u_c^{\sigma_c^{(r)}}) \\
&= \sigma_1^{(r)} \left\{ (\log \gamma_m - \log \gamma_j) \log(1 - \frac{w_m}{w_j}) + (\log \gamma_k - \log \gamma_j) \log(1 - \frac{w_k}{w_j}) \right. \\
&\quad - (\log \gamma_l - \log \gamma_k) \log(1 - \frac{w_l}{w_k}) - (\log \gamma_l - \log \gamma_m) \log(1 - \frac{w_l}{w_m}) \\
&\quad \left. + (\log \gamma_j + \log \gamma_l - \log \gamma_k - \log \gamma_m) \log(1 - \frac{w_j w_l}{w_k w_m}) \right\} \\
&= - \sum_{a=j,k,l,m} \log \gamma_a \left(w_a \frac{\partial W^{(r)}}{\partial w_a} \right) \\
&\quad + \sigma_1^{(r)} (\log \gamma_m - \log \gamma_j) \log \frac{w_k}{w_j} + \sigma_1^{(r)} (\log \gamma_k - \log \gamma_j) \log \frac{w_m}{w_j} \\
&= - \sum_{a=j,k,l,m} \log \gamma_a \left(w_a \frac{\partial W^{(r)}}{\partial w_a} \right) \\
&\quad + \sigma_1^{(r)} p_1^{(r)} \pi i \log u_2^{\sigma_2^{(r)}} + \sigma_1^{(r)} p_2^{(r)} \pi i \log u_1^{\sigma_1^{(r)}} + 2 \log \frac{w_k}{w_j} \log \frac{w_m}{w_j}. \tag{23}
\end{aligned}$$

Using Observation 4.1, (19) and

$$w_b \frac{\partial W}{\partial w_b} \equiv 0 \pmod{2\pi i},$$

we obtain

$$\begin{aligned}
\sum_{r : \text{crossings}} \sum_{a=j,k,l,m} \log \gamma_a \left(w_a \frac{\partial W^{(r)}}{\partial w_a} \right) &= \sum_{b=1}^n \log \gamma_b \left(w_b \frac{\partial W}{\partial w_b} \right) \\
&\equiv \sum_{b=1}^n \left(w_b \frac{\partial W}{\partial w_b} \right) \log w_b \pmod{2\pi^2}. \tag{24}
\end{aligned}$$

From (22), (23) and (24), we have

$$\begin{aligned}
& \frac{1}{2} \sum_{r,c} \sigma_c^{(r)} \left\{ q_c^{(r)} \pi i \log u_c^{\sigma_c^{(r)}} + (p_c^{(r)} \pi i + \log u_c^{\sigma_c^{(r)}}) \log(1 - u_c^{\sigma_c^{(r)}}) \right\} \\
&\equiv - \sum_{b=1}^n \left(w_b \frac{\partial W}{\partial w_b} \right) \log w_b + \sum_r \log u_1^{\sigma_1^{(r)}} \log u_2^{\sigma_2^{(r)}} \pmod{\pi^2}, \tag{25}
\end{aligned}$$

where $c = 1, \dots, 5$ and r is over all crossings.

By definition, the potential function $W(w_1, \dots, w_n)$ is expressed by

$$W(w_1, \dots, w_n) = \sum_{r,c} \sigma_c^{(r)} \left\{ \text{Li}_2(u_c^{\sigma_c^{(r)}}) - \frac{\pi^2}{6} \right\} + \sum_r \log u_1^{\sigma_1^{(r)}} \log u_2^{\sigma_2^{(r)}}. \tag{26}$$

From (25) and (26), we obtain (20) and complete the proof of the first part of Theorem 1.2.

On the other hand, the existence of \mathbf{w}_∞ is guaranteed by [6]. (See [1] for details.) Then we can choose \mathcal{T}_0 the path component containing \mathbf{w}_∞ . This completes the proof of Theorem 1.2.

5 The optimistic limit of the Kashaev invariant

To prove Theorem 1.3, we briefly review the results of [1].

Consider a hyperbolic link L and its non-oriented diagram D . (If D already has an orientation, then we ignore it.) Despite to the colored Jones polynomial version, we assume D does not have any kinks by removing them as in Figure 11. We assign complex variables z_1, \dots, z_g to sides of the diagram. Then we define the potential function of the crossing as in Figure 12.

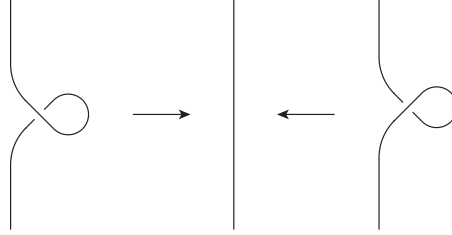


Figure 11: Removing kinks

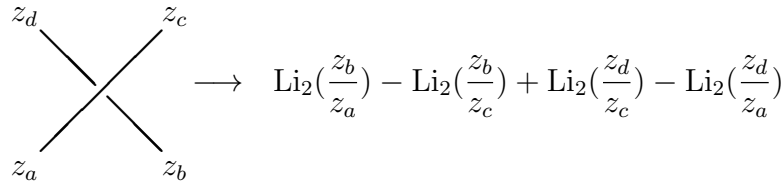


Figure 12: Potential function of a crossing

The potential function $V(z_1, \dots, z_g)$ of the diagram D is defined by the summation of all potential functions of the crossings. Then we define the set \mathcal{H} by

$$\mathcal{H} := \left\{ \exp \left(z_k \frac{\partial V}{\partial z_k} \right) = 1 \mid k = 1, \dots, g \right\}. \quad (27)$$

Let $\mathcal{S} = \{(z_1, \dots, z_g)\}$ be the set of solutions⁶ of \mathcal{H} in \mathbb{C}^g . We always assume $\mathcal{S} \neq \emptyset$. Note that we cannot avoid this assumption because, if the diagram contains the left-hand side of

⁶ As already mentioned in Section 1, we only consider solutions satisfying the condition that, when the potential function V is expressed by $V(z_1, \dots, z_g) = \sum \pm \text{Li}_2(\frac{z_a}{z_b})$, the variable inside the dilogarithms satisfy $\frac{z_a}{z_b} \notin \{0, 1, \infty\}$.

Figure 13, then $\mathcal{S} = \emptyset$. (See [1] for details.) However, this is not true for \mathcal{T} . If the diagram D containing the right-hand side of Figure 13 has a solution (w_1, w_2, w_3, \dots) with $2w_1 \neq w_3$, then the diagram obtained by changing the right-hand side to the left-hand side also has a solution (w_1, \dots, w_6, \dots) . The corresponding solution can be directly calculated by letting $w_6 := w_1$, $w_4 := 2w_1 - w_3$, and w_5 be any non-zero number satisfying $w_5 \neq w_2$ and $w_5 \neq w_4$. (The changes of solutions under the moves of diagram will be discussed in another article the author is preparing.) Remark that this fact shows the colored Jones polynomial version is better than the Kashaev invariant version in the viewpoint of the existence of a solution.

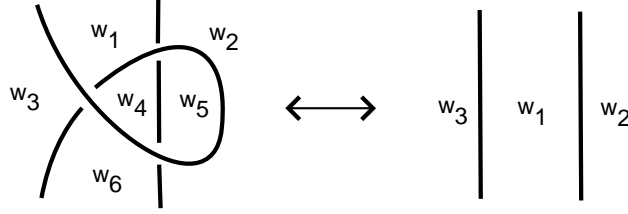


Figure 13: Diagram with $\mathcal{S} = \emptyset$ and $\mathcal{T} \neq \emptyset$

Recall the four-term triangulation of $\mathbb{S}^3 \setminus (L \cup \{\pm\infty\})$ was defined in Section 2. To determine the shape of tetrahedra, we assign shape parameters $\frac{z_b}{z_a}$, $\frac{z_c}{z_b}$, $\frac{z_d}{z_c}$ and $\frac{z_a}{z_d}$ to the horizontal edges $A_k B_k$, $B_k C_k$, $C_k D_k$ and $D_k A_k$ respectively. (See Figure 14.) Then we obtain the following proposition, which was Proposition 1.1 of [1].

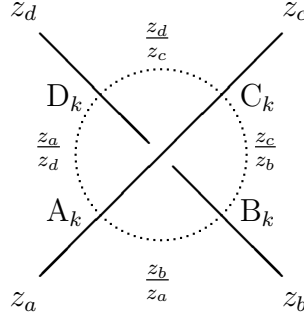


Figure 14: Parametrizing tetrahedra

Proposition 5.1. *For a hyperbolic link L with a fixed diagram, consider the potential function $V(z_1, \dots, z_g)$ of the diagram. Then the set \mathcal{H} defined in (27) becomes the hyperbolicity equations of the four-term triangulation of $\mathbb{S}^3 \setminus (L \cup \{\pm\infty\})$.*

By using Yoshida's construction in Section 4.5 of [6], for a solution $\mathbf{z} = (z_1, \dots, z_g) \in \mathcal{S}$, we can obtain a boundary-parabolic representation

$$\rho_{\mathbf{z}} : \pi_1(\mathbb{S}^3 \setminus (L \cup \{\pm\infty\})) = \pi_1(\mathbb{S}^3 \setminus L) \longrightarrow \mathrm{PSL}(2, \mathbb{C}). \quad (28)$$

For the solution set \mathcal{S} , let \mathcal{S}_j be a path component of \mathcal{S} satisfying $\mathcal{S} = \cup_{j \in J'} \mathcal{S}_j$ for some index set J' . We assume $0 \in J'$ for notational convenience. To obtain well-defined values from the potential function $V(z_1, \dots, z_g)$, we slightly modify it to

$$V_0(z_1, \dots, z_g) := V(z_1, \dots, z_g) - \sum_{k=1}^n \left(z_k \frac{\partial V}{\partial z_k} \right) \log z_k.$$

Then we obtain the main result of [1] as follows:

Theorem 5.2. *Let L be a hyperbolic link with a fixed diagram and $V(z_1, \dots, z_g)$ be the potential function of the diagram. Assume the solution set $\mathcal{S} = \cup_{j \in J'} \mathcal{S}_j$ is not empty. Then, for any $\mathbf{z} \in \mathcal{S}_j$, $V_0(\mathbf{z})$ is constant (depends only on j) and*

$$V_0(\mathbf{z}) \equiv i(\text{vol}(\rho_{\mathbf{z}}) + i \text{cs}(\rho_{\mathbf{z}})) \pmod{\pi^2},$$

where $\rho_{\mathbf{z}}$ is the boundary-parabolic representation in (28). Furthermore, there exists a path component \mathcal{S}_0 of \mathcal{S} satisfying

$$V_0(\mathbf{z}_{\infty}) \equiv i(\text{vol}(L) + i \text{cs}(L)) \pmod{\pi^2},$$

for all $\mathbf{z}_{\infty} \in \mathcal{S}_0$.

We call the value $V_0(\mathbf{z})$ the *optimistic limit of the Kashaev invariant*. Note that it depends on the choice of the diagram and the path component \mathcal{S}_j .

6 Proof of Theorem 1.3

This section is devoted to the proof of Theorem 1.3. Note that it was essentially proved in [2], so we will skip several calculations and refer the results in [2].

To avoid redundant calculations, we change the definition of W_N in Figure 3 to the below:

$$W_N := \text{Li}_2\left(\frac{w_l}{w_m}\right) + \text{Li}_2\left(\frac{w_l}{w_k}\right) - \text{Li}_2\left(\frac{w_j w_l}{w_k w_m}\right) - \text{Li}_2\left(\frac{w_m}{w_j}\right) - \text{Li}_2\left(\frac{w_k}{w_j}\right) + \frac{\pi^2}{6} - \log \frac{w_j}{w_m} \log \frac{w_j}{w_k}. \quad (29)$$

It is possible because, by using the notation in Lemma 3.1 of [2], we know

$$\log \frac{w_j}{w_m} \log \frac{w_j}{w_k} \approx (\log w_j - \log w_m)(\log w_j - \log w_k) \approx \log \frac{w_m}{w_j} \log \frac{w_k}{w_j}.$$

Therefore, changing $\log \frac{w_m}{w_j} \log \frac{w_k}{w_j}$ of W_N to $\log \frac{w_j}{w_m} \log \frac{w_j}{w_k}$ does not have any effect on \mathcal{I} and the optimistic limit $W_0(\mathbf{w})$.

Lemma 6.1. *Fix an oriented diagram D of the hyperbolic link L , which does not have a kink. For a solution $\mathbf{w} = (w_1, \dots, w_n) \in \mathcal{T}$, if the variables w_j, \dots, w_m in Figure 1 satisfy*

$$w_j + w_l \neq w_k + w_m \quad (30)$$

at all crossings, then there exists a solution $\mathbf{z} \in \mathcal{S}$ satisfying $\rho_{\mathbf{w}} = \rho_{\mathbf{z}}$. Inversely, for a solution $\mathbf{z} = (z_1, \dots, z_g) \in \mathcal{S}$, if the variables z_a, \dots, z_d in Figure 1 satisfy

$$z_a \neq z_c \text{ and } z_b \neq z_d \quad (31)$$

at all crossings, then there exists a solution $\mathbf{w} \in \mathcal{T}$ satisfying $\rho_{\mathbf{z}} = \rho_{\mathbf{w}}$.

Proof. For a hyperbolic ideal octahedron in Figure 15, we assign shape parameters $t_1, t_2, t_3, t_4, u_1, u_2, u_3$ and u_4 to the edges CD, DA, AB, BC, CF, DE, AF and BE respectively. Let $u_5 := \frac{1}{u_1 u_3} = \frac{1}{u_2 u_4}$ be the shape parameter of the tetrahedron ABCD assigned to the edges AC and BD.

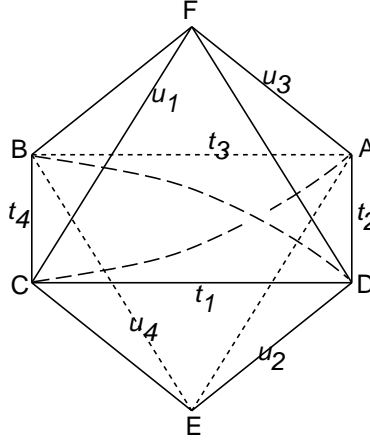


Figure 15: Assignment of variables

Then we obtain the following relations.

$$\begin{cases} t_1 = u_1'' u_2'' u_5', \\ t_2 = u_2' u_3' u_5'', \\ t_3 = u_3'' u_4'' u_5', \\ t_4 = u_4' u_1' u_5'', \end{cases} \quad \begin{cases} u_1 = t_1' t_4'', \\ u_2 = t_1' t_2'', \\ u_3 = t_3' t_2'', \\ u_4 = t_3' t_4'', \\ u_5 = (t_1' t_2'' t_3' t_4'')^{-1}. \end{cases} \quad (32)$$

Now we consider the octahedra placed on the crossings in Figure 7. Note that the five-term triangulation and the four-term triangulation use the same octahedral decomposition of $\mathbb{S}^3 \setminus (L \cup \{\pm\infty\})$, but the subdividing methods are different. Therefore, if we apply (32) to the octahedral decomposition, we can find relations between variables w_1, \dots, w_n and z_1, \dots, z_g . The octahedron on Figure 1(a) (or the one in Figure 7(a)) gives the relations

$$\begin{cases} \frac{z_b}{z_a} = \left(\frac{w_m}{w_j}\right)'' \left(\frac{w_k}{w_j}\right)'' \left(\frac{w_j w_l}{w_k w_m}\right)', & \frac{z_c}{z_b} = \left(\frac{w_k}{w_j}\right)' \left(\frac{w_k}{w_l}\right)' \left(\frac{w_j w_l}{w_k w_m}\right)'', \\ \frac{z_d}{z_c} = \left(\frac{w_k}{w_l}\right)'' \left(\frac{w_m}{w_l}\right)'' \left(\frac{w_j w_l}{w_k w_m}\right)', & \frac{z_a}{z_d} = \left(\frac{w_m}{w_l}\right)' \left(\frac{w_m}{w_j}\right)' \left(\frac{w_j w_l}{w_k w_m}\right)'', \end{cases} \quad (33)$$

and

$$\begin{cases} \frac{w_m}{w_j} = \left(\frac{z_b}{z_a}\right)' \left(\frac{z_a}{z_d}\right)'' , & \frac{w_k}{w_j} = \left(\frac{z_b}{z_a}\right)' \left(\frac{z_c}{z_b}\right)'' , & \frac{w_k}{w_l} = \left(\frac{z_d}{z_c}\right)' \left(\frac{z_c}{z_b}\right)'' , \\ \frac{w_m}{w_l} = \left(\frac{z_d}{z_c}\right)' \left(\frac{z_a}{z_d}\right)'' , & \frac{w_j w_l}{w_k w_m} = \left(\frac{z_a}{z_b}\right)'' \left(\frac{z_b}{z_c}\right)' \left(\frac{z_c}{z_d}\right)'' \left(\frac{z_d}{z_a}\right)' . \end{cases} \quad (34)$$

The octahedron on Figure 1(b) (or the one in Figure 7(b)) gives the relations

$$\begin{cases} \frac{z_b}{z_a} = \left(\frac{w_j}{w_m}\right)' \left(\frac{w_j}{w_k}\right)' \left(\frac{w_k w_m}{w_j w_l}\right)'' , & \frac{z_c}{z_b} = \left(\frac{w_j}{w_k}\right)'' \left(\frac{w_l}{w_k}\right)'' \left(\frac{w_k w_m}{w_j w_l}\right)' , \\ \frac{z_d}{z_c} = \left(\frac{w_l}{w_k}\right)' \left(\frac{w_l}{w_m}\right)' \left(\frac{w_k w_m}{w_j w_l}\right)'' , & \frac{z_a}{z_d} = \left(\frac{w_l}{w_m}\right)'' \left(\frac{w_j}{w_m}\right)'' \left(\frac{w_k w_m}{w_j w_l}\right)' , \end{cases} \quad (35)$$

and

$$\begin{cases} \frac{w_j}{w_m} = \left(\frac{z_a}{z_d}\right)' \left(\frac{z_b}{z_a}\right)'' , & \frac{w_j}{w_k} = \left(\frac{z_c}{z_b}\right)' \left(\frac{z_b}{z_a}\right)'' , & \frac{w_l}{w_k} = \left(\frac{z_c}{z_b}\right)' \left(\frac{z_d}{z_c}\right)'' , \\ \frac{w_l}{w_m} = \left(\frac{z_a}{z_d}\right)' \left(\frac{z_d}{z_c}\right)'' , & \frac{w_k w_m}{w_j w_l} = \left(\frac{z_a}{z_b}\right)' \left(\frac{z_b}{z_c}\right)'' \left(\frac{z_c}{z_d}\right)' \left(\frac{z_d}{z_a}\right)'' . \end{cases} \quad (36)$$

If w_j, \dots, w_m of each crossing is fixed, then we can determine z_a, \dots, z_d using (34) and (36), and the inverse can be done using (33) and (35). Furthermore, if we consider $\mathbf{w} \in \mathbb{CP}^{n-1}$ and $\mathbf{z} \in \mathbb{CP}^{g-1}$, then \mathbf{w} determines \mathbf{z} uniquely, and vice versa.

For the set of equations

$$\begin{cases} \left(\frac{w_m}{w_j}\right)'' \left(\frac{w_k}{w_j}\right)'' \left(\frac{w_j w_l}{w_k w_m}\right)' \neq 1, & \left(\frac{w_k}{w_j}\right)' \left(\frac{w_k}{w_l}\right)' \left(\frac{w_j w_l}{w_k w_m}\right)'' \neq 1, \\ \left(\frac{w_k}{w_l}\right)'' \left(\frac{w_m}{w_l}\right)'' \left(\frac{w_j w_l}{w_k w_m}\right)' \neq 1, & \left(\frac{w_m}{w_l}\right)' \left(\frac{w_m}{w_j}\right)' \left(\frac{w_j w_l}{w_k w_m}\right)'' \neq 1, \end{cases} \quad (37)$$

in (33) and

$$\begin{cases} \left(\frac{w_j}{w_m}\right)' \left(\frac{w_j}{w_k}\right)' \left(\frac{w_k w_m}{w_j w_l}\right)'' \neq 1, & \left(\frac{w_j}{w_k}\right)'' \left(\frac{w_l}{w_k}\right)'' \left(\frac{w_k w_m}{w_j w_l}\right)' \neq 1, \\ \left(\frac{w_l}{w_k}\right)' \left(\frac{w_l}{w_m}\right)' \left(\frac{w_k w_m}{w_j w_l}\right)'' \neq 1, & \left(\frac{w_l}{w_m}\right)'' \left(\frac{w_j}{w_m}\right)'' \left(\frac{w_k w_m}{w_j w_l}\right)' \neq 1, \end{cases} \quad (38)$$

in (35), direct calculation shows (37), (38) and (30) are equivalent each other. Therefore, (30) guarantees the determined \mathbf{z} is a solution $\mathbf{z} \in \mathcal{S}$.

Also, for the set of equations

$$\begin{cases} \left(\frac{z_b}{z_a}\right)' \left(\frac{z_a}{z_d}\right)'' \neq 1, & \left(\frac{z_b}{z_a}\right)' \left(\frac{z_c}{z_b}\right)'' \neq 1, & \left(\frac{z_d}{z_c}\right)' \left(\frac{z_c}{z_b}\right)'' \neq 1, \\ \left(\frac{z_d}{z_c}\right)' \left(\frac{z_a}{z_d}\right)'' \neq 1, & \left(\frac{z_a}{z_b}\right)'' \left(\frac{z_b}{z_c}\right)' \left(\frac{z_c}{z_d}\right)'' \left(\frac{z_d}{z_a}\right)' \neq 1, \end{cases} \quad (39)$$

in (34) and

$$\begin{cases} \left(\frac{z_a}{z_d}\right)' \left(\frac{z_b}{z_a}\right)'' \neq 1, & \left(\frac{z_c}{z_b}\right)' \left(\frac{z_b}{z_a}\right)'' \neq 1, & \left(\frac{z_c}{z_b}\right)' \left(\frac{z_d}{z_c}\right)'' \neq 1, \\ \left(\frac{z_a}{z_d}\right)' \left(\frac{z_d}{z_c}\right)'' \neq 1, & \left(\frac{z_a}{z_b}\right)' \left(\frac{z_b}{z_c}\right)'' \left(\frac{z_c}{z_d}\right)' \left(\frac{z_d}{z_a}\right)'' \neq 1 \end{cases} \quad (40)$$

in (36), direct calculation shows (39), (40) and (31) are equivalent each other. Therefore, (31) guarantees the determined \mathbf{w} is a solution $\mathbf{w} \in \mathcal{T}$.

Finally, if \mathbf{z} and \mathbf{w} are related as above, then they determine the same octahedral decomposition and the same developing map. Therefore, we conclude $\rho_{\mathbf{z}} = \rho_{\mathbf{w}}$. \square

Let $D(z) := \text{Im Li}_2(z) + \log |z| \arg(1 - z)$ be the Bloch-Wigner function for $z \in \mathbb{C} \setminus \{0, 1\}$. It is a well-known fact that $D(z) = \text{vol}(T_z)$, where T_z is the hyperbolic ideal tetrahedron with the shape parameter z . Therefore, from Figure 15, we obtain

$$D(t_1) + D(t_2) + D(t_3) + D(t_4) = D(u_1) + D(u_2) + D(u_3) + D(u_4) + D(u_5). \quad (41)$$

Note that the variables $t_1, \dots, t_4, u_1, \dots, u_5$ satisfying (32) determine a hyperbolic ideal octahedron in Figure 15, so (32) guarantees (41).

Lemma 6.2. *Let $t_1, t_2, t_3, t_4, u_1, u_2, u_3, u_4, u_5 \notin \{0, 1, \infty\}$ be the shape parameters defined in the hyperbolic octahedron in Figure 15, which satisfies (32) and (41). Then the following identities hold for any choice of log-branch modulo $4\pi^2$.*

$$\begin{aligned} & \text{Li}_2(t_1) - \text{Li}_2\left(\frac{1}{t_2}\right) + \text{Li}_2(t_3) - \text{Li}_2\left(\frac{1}{t_4}\right) \\ & \equiv \text{Li}_2(u_1) + \text{Li}_2(u_2) - \text{Li}_2\left(\frac{1}{u_3}\right) - \text{Li}_2\left(\frac{1}{u_4}\right) + \text{Li}_2(u_5) - \frac{\pi^2}{6} + \log u_1 \log u_2 \\ & \quad - \left(-\log(1 - t_1) + \log\left(1 - \frac{1}{t_4}\right)\right) \log u_2 - \left(-\log(1 - t_1) + \log\left(1 - \frac{1}{t_2}\right)\right) \log u_1 \\ & \quad + \left(-\log(1 - t_1) + \log\left(1 - \frac{1}{t_4}\right)\right) \log(1 - u_1) + \left(-\log(1 - t_1) + \log\left(1 - \frac{1}{t_2}\right)\right) \log(1 - u_2) \\ & \quad + \left(-\log(1 - t_3) + \log\left(1 - \frac{1}{t_2}\right)\right) \log\left(1 - \frac{1}{u_3}\right) + \left(-\log(1 - t_3) + \log\left(1 - \frac{1}{t_4}\right)\right) \log\left(1 - \frac{1}{u_4}\right) \\ & \quad + \left(\log(1 - t_1) - \log\left(1 - \frac{1}{t_2}\right) + \log(1 - t_3) - \log\left(1 - \frac{1}{t_4}\right)\right) \log(1 - u_5) \end{aligned}$$

$$\begin{aligned}
&\equiv \text{Li}_2(u_1) - \text{Li}_2\left(\frac{1}{u_2}\right) - \text{Li}_2\left(\frac{1}{u_3}\right) + \text{Li}_2(u_4) - \text{Li}_2\left(\frac{1}{u_5}\right) + \frac{\pi^2}{6} - \log u_2 \log u_3 \\
&\quad + \left(-\log(1-t_3) + \log(1-\frac{1}{t_2})\right) \log u_2 + \left(-\log(1-t_1) + \log(1-\frac{1}{t_2})\right) \log u_3 \\
&\quad + \left(-\log(1-t_1) + \log(1-\frac{1}{t_4})\right) \log(1-u_1) + \left(-\log(1-t_1) + \log(1-\frac{1}{t_2})\right) \log(1-\frac{1}{u_2}) \\
&\quad + \left(-\log(1-t_3) + \log(1-\frac{1}{t_2})\right) \log(1-\frac{1}{u_3}) + \left(-\log(1-t_3) + \log(1-\frac{1}{t_4})\right) \log(1-u_4) \\
&\quad + \left(\log(1-t_1) - \log(1-\frac{1}{t_2}) + \log(1-t_3) - \log(1-\frac{1}{t_4})\right) \log(1-\frac{1}{u_5}) \pmod{4\pi^2}.
\end{aligned}$$

Proof. See the proof of Lemma 5.1 in [2]. □

Let $\mathbf{w} \in \mathcal{T}$ and $\mathbf{z} \in \mathcal{S}$ be the corresponding pair in Lemma 6.1. To prove

$$V_0(\mathbf{z}) \equiv W_0(\mathbf{w}) \pmod{4\pi^2}, \quad (42)$$

we consider the two cases of the crossing with parameters $z_a, \dots, z_d, w_j, \dots, w_m$ in Figure 1.

For the case of Figure 1(a), we let $t_1 = \frac{z_b}{z_a}$, $t_2 = \frac{z_c}{z_b}$, $t_3 = \frac{z_d}{z_c}$, $t_4 = \frac{z_a}{z_d}$, $u_1 = \frac{w_m}{w_j}$, $u_2 = \frac{w_k}{w_j}$, $u_3 = \frac{w_k}{w_l}$, $u_4 = \frac{w_m}{w_l}$ and $u_5 = \frac{w_j w_l}{w_k w_m}$ so that (32) satisfies. Then the potential function of a crossing defined in Figure 12 is expressed by

$$V_P(z_a, \dots, z_d) := \text{Li}_2(t_1) - \text{Li}_2\left(\frac{1}{t_2}\right) + \text{Li}_2(t_3) - \text{Li}_2\left(\frac{1}{t_4}\right),$$

and the potential function of a positive crossing defined in Figure 3(a) is expressed by

$$\begin{aligned}
&W_P(w_j, w_k, w_l, w_m) \\
&= \text{Li}_2(u_1) + \text{Li}_2(u_2) - \text{Li}_2\left(\frac{1}{u_3}\right) - \text{Li}_2\left(\frac{1}{u_4}\right) + \text{Li}_2(u_5) - \frac{\pi^2}{6} + \log u_1 \log u_2.
\end{aligned}$$

Using Lemma 6.2, we can calculate

$$\begin{aligned}
V_{P0} - W_{P0} &\equiv -(\log w_j - \log w_m) \log z_a - (\log w_k - \log w_j) \log z_b \\
&\quad + (\log w_k - \log w_l) \log z_c + (\log w_l - \log w_m) \log z_d \pmod{4\pi^2}. \quad (43)
\end{aligned}$$

(The details are in (41)–(42) and the following paragraphs of Section 5 in [2]. Note that, in [2], we denoted V_P and W_P by $X(z_a, \dots, z_d)$ and $P_1(w_j, \dots, w_m)$ respectively.)

For the case of Figure 1(b), we let $t_1 = \frac{z_a}{z_d}$, $t_2 = \frac{z_b}{z_a}$, $t_3 = \frac{z_c}{z_b}$, $t_4 = \frac{z_d}{z_c}$, $u_1 = \frac{w_l}{w_m}$, $u_2 = \frac{w_j}{w_m}$, $u_3 = \frac{w_j}{w_k}$, $u_4 = \frac{w_l}{w_k}$ and $u_5 = \frac{w_k w_m}{w_j w_l}$ so that (32) satisfies. Then the potential function of a crossing defined in Figure 12 is expressed by

$$V_N(z_a, \dots, z_d) := \text{Li}_2(t_1) - \text{Li}_2\left(\frac{1}{t_2}\right) + \text{Li}_2(t_3) - \text{Li}_2\left(\frac{1}{t_4}\right),$$

and the potential function of a negative crossing defined in (29) is expressed by

$$\begin{aligned} W_N(w_j, w_k, w_l, w_m) \\ = \text{Li}_2(u_1) - \text{Li}_2\left(\frac{1}{u_2}\right) - \text{Li}_2\left(\frac{1}{u_3}\right) + \text{Li}_2(u_4) - \text{Li}_2\left(\frac{1}{u_5}\right) + \frac{\pi^2}{6} - \log u_2 \log u_3. \end{aligned}$$

Using Lemma 6.2, we can calculate

$$\begin{aligned} V_{N0} - W_{N0} \equiv & -(\log w_j - \log w_m) \log z_a - (\log w_k - \log w_j) \log z_b \\ & + (\log w_k - \log w_l) \log z_c + (\log w_l - \log w_m) \log z_d \pmod{4\pi^2}. \end{aligned} \quad (44)$$

Note that the right-hand sides of (43) and (44) coincide. We can deduce the general rule of these equations using Figure 16.

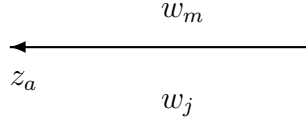


Figure 16: Side assigned by z_a

For the side with z_a in Figure 16, when it goes out of a crossing, the contribution to (43) or (44) of the crossing is

$$-(\log w_j - \log w_m) \log z_a,$$

and when it goes into a crossing, the contribution is

$$+(\log w_j - \log w_m) \log z_a.$$

Therefore, if we consider the whole crossings of the link diagram, the right-hand sides of (43) or (44) at all crossings are cancelled out and we obtain (42). This completes the proof of Theorem 1.3.

7 Example of the twist knots

In this section, we apply Theorem 1.3 to the example of the twist knot in Section 6 of [1] and show several numerical results. For the calculations, we assume the principal branch of logarithm. Also we use the definition of W_N in Figure 3(b).

Let T_n ($n \geq 1$) be the twist knot with $n + 3$ crossings in Figure 17. For example, T_1 is the figure-eight knot 4_1 and T_2 is the 5_2 knot. We follow the orientations in Figure 17.

We assign variables $a, b, x_0, \dots, x_{n+1}, y_0, \dots, y_{n+1}$ to the sides and $c, d, e, w_0, \dots, w_{n+1}$ to the regions of Figure 17 respectively. Let

$$A_k := \text{Li}_2\left(\frac{c}{w_k}\right) + \text{Li}_2\left(\frac{c}{w_{k+1}}\right) - \text{Li}_2\left(\frac{ce}{w_k w_{k+1}}\right) - \text{Li}_2\left(\frac{w_k}{e}\right) - \text{Li}_2\left(\frac{w_{k+1}}{e}\right) + \frac{\pi^2}{6} - \log \frac{w_k}{e} \log \frac{w_{k+1}}{e},$$

$$B_k := \text{Li}_2\left(\frac{e}{w_k}\right) + \text{Li}_2\left(\frac{e}{w_{k+1}}\right) - \text{Li}_2\left(\frac{ce}{w_k w_{k+1}}\right) - \text{Li}_2\left(\frac{w_k}{c}\right) - \text{Li}_2\left(\frac{w_{k+1}}{c}\right) + \frac{\pi^2}{6} - \log \frac{w_k}{c} \log \frac{w_{k+1}}{c},$$

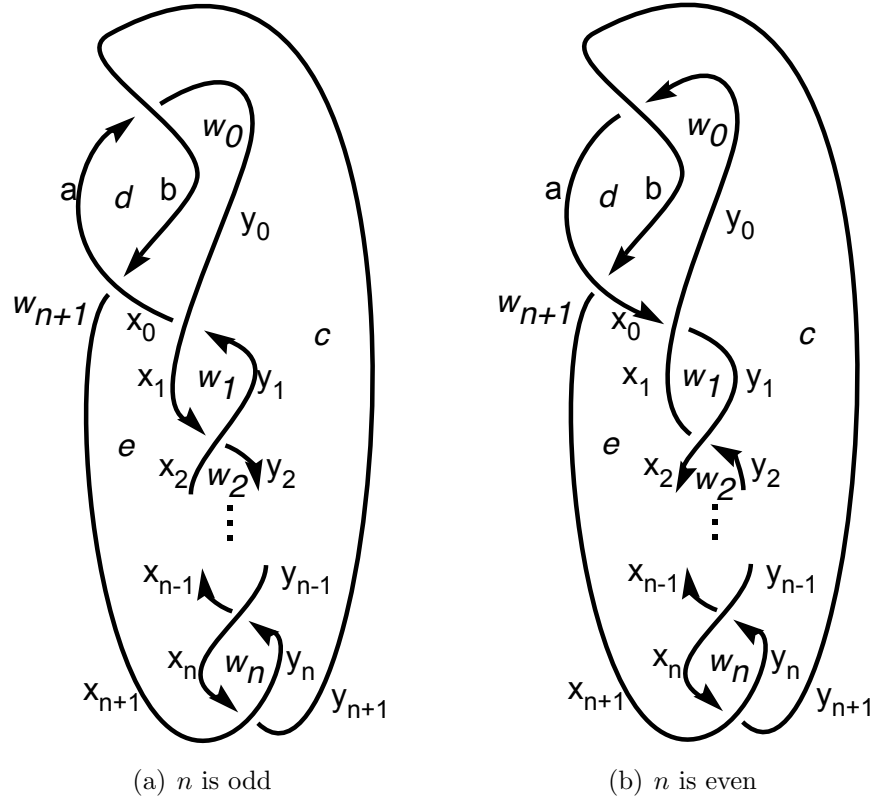


Figure 17: Twist knot T_n

for $k = 0, 1, \dots, n$. If n is odd, the potential function $W(T_n; c, d, e, w_0, \dots, w_{n+1})$ of Figure 17(a) is

$$\begin{aligned}
& W(T_n; c, d, e, w_0, \dots, w_{n+1}) \\
&= \left\{ -\text{Li}_2\left(\frac{w_{n+1}}{c}\right) - \text{Li}_2\left(\frac{w_{n+1}}{d}\right) + \text{Li}_2\left(\frac{w_0 w_{n+1}}{c d}\right) + \text{Li}_2\left(\frac{c}{w_0}\right) + \text{Li}_2\left(\frac{d}{w_0}\right) \right. \\
&\quad \left. - \frac{\pi^2}{6} + \log \frac{c}{w_0} \log \frac{d}{w_0} \right\} \\
&+ \left\{ -\text{Li}_2\left(\frac{w_0}{d}\right) - \text{Li}_2\left(\frac{w_0}{e}\right) + \text{Li}_2\left(\frac{w_0 w_{n+1}}{d e}\right) + \text{Li}_2\left(\frac{d}{w_{n+1}}\right) + \text{Li}_2\left(\frac{e}{w_{n+1}}\right) \right. \\
&\quad \left. - \frac{\pi^2}{6} + \log \frac{d}{w_{n+1}} \log \frac{e}{w_{n+1}} \right\} \\
&+ \sum_{k=0}^{(n-1)/2} (A_{2k} + B_{2k+1}),
\end{aligned}$$

and if n is even, the potential function $W(T_n; c, d, e, w_0, \dots, w_{n+1})$ of Figure 17(b) is

$$\begin{aligned}
& W(T_n; c, d, e, w_0, \dots, w_{n+1}) \\
&= \left\{ \operatorname{Li}_2\left(\frac{c}{w_0}\right) + \operatorname{Li}_2\left(\frac{c}{w_{n+1}}\right) - \operatorname{Li}_2\left(\frac{cd}{w_0 w_{n+1}}\right) - \operatorname{Li}_2\left(\frac{w_0}{d}\right) - \operatorname{Li}_2\left(\frac{w_{n+1}}{d}\right) \right. \\
&\quad \left. + \frac{\pi^2}{6} - \log \frac{w_0}{d} \log \frac{w_{n+1}}{d} \right\} \\
&+ \left\{ \operatorname{Li}_2\left(\frac{d}{w_0}\right) + \operatorname{Li}_2\left(\frac{d}{w_{n+1}}\right) - \operatorname{Li}_2\left(\frac{de}{w_0 w_{n+1}}\right) - \operatorname{Li}_2\left(\frac{w_0}{e}\right) - \operatorname{Li}_2\left(\frac{w_{n+1}}{e}\right) \right. \\
&\quad \left. + \frac{\pi^2}{6} - \log \frac{w_0}{e} \log \frac{w_{n+1}}{e} \right\} \\
&+ B_0 + \sum_{k=1}^{n/2} (A_{2k-1} + B_{2k}).
\end{aligned}$$

In Section 6 of [1], we chose $(a, b, x_0, \dots, x_{n+1}, y_0, \dots, y_{n+1})$ by

$$\begin{aligned}
& a = 2, \quad b = -1, \quad x_0 = t, \quad y_0 = 1 + \frac{2}{t}, \quad x_1 = \frac{t(t+2)}{t^2 - 4t + 8}, \quad y_1 = \frac{4}{t}, \\
& x_{k+1} = \frac{x_k y_k}{-x_{k-1} + x_k + y_k}, \quad y_{k+1} = x_k + y_k - \frac{x_k y_k}{y_{k-1}}, \quad x_{n+1} = 3, \quad y_{n+1} = 1,
\end{aligned}$$

where $k = 1, \dots, n-1$, and t is a solution of the defining equation in Table 1. All the solutions t of the defining equation determine the solutions in \mathcal{S} and the corresponding representation

$$\rho(T_n)(t) : \pi_1(\mathbb{S}^3 \setminus T_n) \longrightarrow \operatorname{PSL}(2, \mathbb{C}).$$

n	Defining equation of t
1	$16 - 12t + 3t^2 = 0$
2	$-64 + 80t - 40t^2 + 7t^3 = 0$
3	$256 - 448t + 336t^2 - 120t^3 + 17t^4 = 0$
4	$-2048 + 4608t - 4608t^2 + 2464t^3 - 696t^4 + 82t^5 = 0$
5	$4096 - 11264t + 14080t^2 - 9984t^3 + 4192t^4 - 980t^5 + 99t^6 = 0$

Table 1: Defining equation of t for $n = 1, \dots, 5$

Using the equations (34) and (36), we can express $(c, d, e, w_0, \dots, w_{n+1})$ in terms of t . Specifically, the $(k+2)$ -th crossing (in the order from top to bottom) in Figure 17 becomes Figure 18 and it determines

$$\frac{e}{w_k} = \left(\frac{y_k}{x_k} \right)' \left(\frac{x_k}{x_{k-1}} \right)'',$$

for $k = 1, \dots, n+1$. The first crossing in Figure 17 gives an equation of c

$$\frac{c}{w_{n+1}} = \left(\frac{a}{y_{n+1}} \right)' \left(\frac{y_{n+1}}{y_0} \right)' = \frac{2}{t}.$$

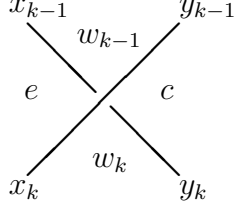


Figure 18: The $(k+2)$ -th crossing for $k = 1, \dots, n+1$

The second crossing in Figure 17 gives more simple equation of w_{n+1}

$$\frac{e}{w_{n+1}} = \left(\frac{x_{n+1}}{a} \right)' \left(\frac{x_0}{x_{n+1}} \right)'' = -\frac{2(t-3)}{t},$$

and other equations of d and w_0

$$\frac{d}{w_{n+1}} = \left(\frac{x_{n+1}}{a} \right)' \left(\frac{a}{b} \right)'' = -3, \quad \frac{e}{w_0} = \left(\frac{b}{x_0} \right)' \left(\frac{x_0}{x_{n+1}} \right)'' = \frac{t-3}{t+1}.$$

Therefore, after choosing $e = 1$, we can express $(c, d, e, w_0, \dots, w_{n+1})$ in terms of t by

$$c = -\frac{1}{t-3}, \quad d = \frac{3t}{2(t-3)}, \quad e = 1, \quad w_0 = \frac{t+1}{t-3}, \quad w_k = \left(\frac{x_k}{y_k} \right)'' \left(\frac{x_{k-1}}{x_k} \right)',$$

for $k = 1, \dots, n+1$. The exact expression of w_k for $k = 1, \dots, 6$ is in Table 2.

k	w_k
0	$(1+t)/(-3+t)$
1	$-(16+t^2)/((-3+t)t^2)$
2	$(256-256t+112t^2-16t^3-3t^4+t^5)/((-3+t)t^4)$
3	$(-4096+8192t-7424t^2+3584t^3-864t^4+32t^5+27t^6-4t^7)/((-3+t)t^6)$
4	$(65536-196608t+274432t^2-225280t^3+115456t^4-35584t^5+5152t^6+320t^7-231t^8+25t^9)/((-3+t)t^8)$
5	$(-1048576+4194304t-7929856t^2+9175040t^3-7094272t^4+3760128t^5-1337088t^6+287232t^7-21232t^8-6048t^9+1751t^{10}-144t^{11})/((-3+t)t^{10})$
6	$(16777216-83886080t+200278016t^2-298844160t^3+307822592t^4-228524032t^5+123846656t^6-48324608t^7+12842496t^8-1930752t^9-2544t^{10}+66288t^{11}-12587t^{12}+841t^{13})/((-3+t)t^{12})$

Table 2: Expressions of w_k in terms of t for $k = 1, \dots, 6$

For the solutions t of the defining equations, the numerical values of the corresponding optimistic limits

$$W_0(T_n)(t) \equiv i(\text{vol}(\rho(T_n)(t)) + i \text{cs}(\rho(T_n)(t))) \pmod{\pi^2},$$

for $n = 1, \dots, 5$, are in Table 3. Note that these values exactly coincide with the optimistic limits of Kashaev invariants in Table 3 of [1].

n	t	$W_0(T_n)(t) \equiv i(\text{vol}(\rho(T_n)(t)) + i \text{cs}(\rho(T_n)(t)))$
1	$t = 2 + 1.1547...i$	$i(2.0299... + 0i)$
	$t = 2 - 1.1547...i$	$i(-2.0299... + 0i)$
2	$t = 1.4587... + 1.0682...i$	$i(2.8281... + 3.0241...i)$
	$t = 1.4587... - 1.0682...i$	$i(-2.8281... + 3.0241...i)$
	$t = 2.7969...$	$i(0 - 1.1135...i)$
3	$t = 1.2631... + 1.0347...i$	$i(3.1640... + 6.7907...i)$
	$t = 1.2631... - 1.0347...i$	$i(-3.1640... + 6.7907...i)$
	$t = 2.2664... + 0.7158...i$	$i(1.4151... + 0.2110...i)$
	$t = 2.2664... - 0.7158...i$	$i(-1.4151... + 0.2110...i)$
4	$t = 1.1713... + 1.0202...i$	$i(3.3317... + 10.9583...i)$
	$t = 1.1713... - 1.0202...i$	$i(-3.3317... + 10.9583...i)$
	$t = 1.8097... + 0.9073...i$	$i(2.2140... + 1.8198...i)$
	$t = 1.8097... - 0.9073...i$	$i(-2.2140... + 1.8198...i)$
	$t = 2.5257...$	$i(0 - 0.8822...i)$
5	$t = 1.1208... + 1.0129...i$	$i(3.4272... + 15.3545...i)$
	$t = 1.1208... - 1.0129...i$	$i(-3.4272... + 15.3545...i)$
	$t = 1.5498... + 0.9676...i$	$i(2.6560... + 4.6428...i)$
	$t = 1.5498... - 0.9676...i$	$i(-2.6560... + 4.6428...i)$
	$t = 2.2789... + 0.4876...i$	$i(1.1087... - 0.2581...i)$
	$t = 2.2789... - 0.4876...i$	$i(-1.1087... - 0.2581...i)$

Table 3: Values of $W_0(T_n)(t)$ for $n = 1, \dots, 5$

Acknowledgments The author is supported by POSCO TJ Park foundation. He appreciates Hyuk Kim and Seonhwa Kim for discussions and suggestions on this work.

References

- [1] J. Cho, H. Kim, and S. Kim. Optimistic limits of kashaev invariants and complex volumes of hyperbolic links. <http://arxiv.org/abs/1301.6219>.
- [2] J. Cho and J. Murakami. Optimistic limits of the colored Jones polynomials. <http://arxiv.org/abs/1009.3137>, to appear in J. Korean Math. Soc.

- [3] J. Cho and J. Murakami. The complex volumes of twist knots via colored Jones polynomials. *J. Knot Theory Ramifications*, 19(11):1401–1421, 2010.
- [4] J. Cho, J. Murakami, and Y. Yokota. The complex volumes of twist knots. *Proc. Amer. Math. Soc.*, 137(10):3533–3541, 2009.
- [5] R. M. Kashaev. The hyperbolic volume of knots from the quantum dilogarithm. *Lett. Math. Phys.*, 39(3):269–275, 1997.
- [6] F. Luo, S. Tillmann, and T. Yang. Thurston’s spinning construction and solutions to the hyperbolic gluing equations for closed hyperbolic 3-manifolds. <http://arxiv.org/abs/1004.2992>.
- [7] H. Murakami. Optimistic calculations about the Witten-Reshetikhin-Turaev invariants of closed three-manifolds obtained from the figure-eight knot by integral Dehn surgeries. *Sūrikaiseikikenkyūsho Kōkyūroku*, (1172):70–79, 2000. Recent progress towards the volume conjecture (Japanese) (Kyoto, 2000).
- [8] H. Murakami and J. Murakami. The colored Jones polynomials and the simplicial volume of a knot. *Acta Math.*, 186(1):85–104, 2001.
- [9] K. Ohnuki. The colored Jones polynomials of 2-bridge link and hyperbolicity equations of its complements. *J. Knot Theory Ramifications*, 14(6):751–771, 2005.
- [10] H. Segerman and S. Tillmann. Pseudo-developing maps for ideal triangulations I: essential edges and generalised hyperbolic gluing equations. In *Topology and geometry in dimension three*, volume 560 of *Contemp. Math.*, pages 85–102. Amer. Math. Soc., Providence, RI, 2011.
- [11] Y. Yokota. On the complex volume of hyperbolic knots. *J. Knot Theory Ramifications*, 20(7):955–976, 2011.
- [12] C. K. Zickert. The volume and Chern-Simons invariant of a representation. *Duke Math. J.*, 150(3):489–532, 2009.

Department of Mathematics, Korea Institute for Advanced Study(KIAS), 85 Hoegiro,
Dongdaemun-gu, Seoul 130-722, Republic of Korea

E-mail: dol0425@gmail.com